111-61
63228

P-61

FORTRAN Program for Analyzing Ground-Based Radar Data: Usage and Derivations, Version 6.2

Edward A. Haering, Jr., and
Stephen A. Whitmore

FORTRAN Program for Analyzing Ground-Based Radar Data: Usage and Derivations, Version 6.2

Edward A. Haering, Jr., and
Stephen A. Whitmore
Dryden Flight Research Center
Edwards, California

CONTENTS

ABSTRACT

A postflight FORTRAN program called "radar" reads and analyzes ground-based radar data. The output includes position, velocity, and acceleration parameters. Airdata parameters are also provided if atmospheric characteristics are input. This program can read data from any radar in three formats. Geocentric Cartesian position can also be used as input, which may be from an inertial navigation or Global Positioning System. Options include spike removal, data filtering, and atmospheric refraction corrections. Atmospheric refraction can be corrected using the quick White Sands method or the gradient refraction method, which allows accurate analysis of very low elevation angle and long-range data. Refraction properties are extrapolated from surface conditions, or a measured profile may be input. Velocity is determined by differentiating position. Accelerations are determined by differentiating velocity. This paper describes the algorithms used, gives the operational details, and discusses the limitations and errors of the program. Appendixes A through E contain the derivations for these algorithms. These derivations include an improvement in speed to the exact solution for geodetic altitude, an improved algorithm over earlier versions for determining scale height, a truncation algorithm for speeding up the gradient refraction method, and a refinement of the coefficients used in the White Sands method for Edwards AFB, California. Appendix G contains the nomenclature.

INTRODUCTION

One way to determine the trajectory of a flight vehicle is to analyze the ground-based, radar-tracking data. The radar measures range to the vehicle, azimuth of the vehicle from true north, and elevation angle of the vehicle above the local horizon. These measurements need to be filtered and corrected for atmospheric refraction. Then, geometric principles can be applied to convert these data into such familiar forms as latitude, longitude, and altitude. Next, derivatives can be taken to determine velocity and acceleration. These quantities are easily calculated in real time at the radar site, and the results are sufficiently accurate for many applications. To achieve these calculations in real time, however, certain assumptions are made regarding the structure of the atmosphere. These assumptions may introduce errors in the refraction corrections. Often for the high accuracies required for flight research, analyzing the atmospheric parameters after the flight and then using the results for refraction corrections is necessary. The process of analyzing the atmosphere can be quite involved[1] and will not be available in real time in the foreseeable future. Using atmospheric data gathered and analyzed before radar-tracking time suffers from temporal variations of the atmosphere.[1] An added benefit of analyzing the radar data after the flight using an atmospheric analysis is that such airdata parameters as Mach number, true airspeed, and pressure altitude may be accurately determined.

A postflight FORTRAN program called "radar" reads and analyzes ground-based radar data from any radar site. This program provides Earth relative position, velocity, and acceleration parameters. Airdata parameters are also provided if atmospheric characteristics are input. This program reads data from the NASA Dryden Flight Research Center (NASA Dryden), Edwards, California, Flight Data Access System (FDAS)[*]; the encoded 9-track radar tape from the Army-Navy/Fixed Position System (AN/FPS-16) radars at Edwards AFB, California; or binary range, azimuth, and elevation angle data from any other radar. Cartesian position with respect to the center of the Earth can also be used as input. This position may be from an inertial navigation system or the Global Positioning System (GPS). Output from this program is in NASA Dryden compressed format.[2] As an option, the output can also be written in binary format. Program options include spike removal, data filtering, and atmospheric refraction corrections. Atmospheric refraction can be corrected by using either the quick White Sands method[3], which is inaccurate at low elevation angles, or the accurate, but computationally slow, gradient refraction method.[4]

---

*Maine, Richard E., User's Manual for GetFdas, Version 0.72, Apr. 30, 1993, NASA Dryden working paper.

Refraction properties are either extrapolated from surface conditions or determined from a user-supplied table of refraction as a function of altitude. The program models the Earth as an ellipsoid. Velocity is determined by differentiating position, and accelerations are determined by differentiating velocity.

This paper describes the algorithms, operational details, limitations, and errors for version 6.2 of "radar." Although earlier versions have existed for decades, this paper is the first time the program has been documented. Appendixes A through E contain the derivations for these algorithms. These derivatives include an improvement in speed to the exact solution for geometric ellipsoid altitude, an improved algorithm over earlier versions for determining scale height, a truncation algorithm for speeding up the gradient refraction method, and a refinement of coefficients used in the White Sands method for Edwards AFB, California. Appendixes A through E are universally applicable. Appendix F is specific to the program used at NASA Dryden. The nomenclature is given in appendix G.

METHOD DESCRIPTIONS

The methods for analyzing radar data are discussed next. These methods include geodetics, refraction corrections, spike removal and filtering, velocity and acceleration determination, and Earth relative and airdata parameters.

Geodetics

The basic information provided by a ground-based radar is time-referenced range, azimuth, and elevation angle to the vehicle. After various corrections are applied to these three quantities, the position of the vehicle with respect to the radar site can be calculated. Location of the radar site with respect to the center of the Earth can also be calculated. Adding these two vector positions yields the position of the vehicle with respect to the center of the Earth. The equations used to determine position are derived in appendix A.

The Earth is modeled as an ellipse of revolution, otherwise known as an ellipsoid. Table 1 lists the semimajor and semiminor axes of this ellipse, a and b, in several systems. The World Geodetic Survey (WGS) 84 is used by most radar systems in the United States and is included in this table. Determining the altitude and latitude of the vehicle about an ellipsoid requires somewhat complex calculations, and these calculations are shown in appendix B. An improvement to the exact solution for determining altitude, which results in reduced computations, is also presented.

Note that the algorithms in appendix B are used to calculate ellipsoid altitude which is different from geoid altitude. Geoid altitude is the altitude above mean sea level (m.s.l.). Because of mass irregularities of the Earth, the geoid is a highly irregular surface. For the continental United States, the geoid separation (ellipsoid altitude minus geoid altitude) is a negative number and is approximately –100 ft for radar 34 at Edwards AFB, California, using the WGS 84 system. Because most users desire geoid altitude, the ellipsoid altitude is biased by the radar site geoid separation to give geoid altitude. Another bias to altitude can be input to approximate the geoid separation change for flights great distances from the radar site. This method works well when the vehicle travels over an area where

Table 1. Ellipsoid Earth models.

Model	Semimajor axis a, ft	Semiminor axis b, ft	$a/(a-b)$
WGS 84	20925604.47	20855444.88	298.25722043
WGS 72	20925639.76	20855480.71	298.26002261
"radar", version 4.0	20925832.00	20854892.00	294.97930764

geoid separation is relatively constant but is less effective for trajectories over long distances. A future improvement to this program would be an analytical calculation or database lookup of geoid separation as a function of latitude and longitude to adjust ellipsoid altitude to altitude above mean sea level.

Refraction Corrections

A radar unit measures the time a pulse of electromagnetic energy takes to travel from the radar antenna to the vehicle and return to its originating location. The initial assumption is that the pulse travels at the speed of light in a vacuum, so the range to the vehicle is easily calculated. The angle at which the antenna is pointed above the local horizontal is the measured elevation angle. The speed of light through the atmosphere is not the same as it is through a vacuum because it is affected by pressure, temperature, and humidity. Because these three quantities vary with altitude, the speed of light varies with altitude. The variation of the speed of light with altitude also causes the beam of light to bend. For example, consider two parallel beams of light in the atmosphere that are nearly horizontal with the Earth and at slightly different altitudes. The speed of light through the atmosphere is c_o/η, where c_o is the speed of light in a vacuum, and η is the index of refraction. Because η generally decreases with altitude, and c_o is a constant, the upper beam travels slightly farther than the lower beam in the same amount of time. In this manner, the wave front has bent downward. This bending effect occurs for each incremental segment of the radar beam.

Figure 1 shows the effect of a nonhomogeneous atmosphere on a radar beam. The radar beam follows a curved path, and most of the curvature occurs near the ground. The true straight line range to the vehicle is less than the measured range along the curved radar beam path. In addition, the true elevation angle is less than the measured elevation angle. This effect of atmospheric refraction is the greatest source of error and also the most difficult to correct.

To correct for refraction, the properties of the atmosphere as a function of altitude must be determined. An easy method is to measure the properties at the radar site and then to extrapolate values at increased altitudes. Because of the extrapolation, this method is the least accurate. A more nearly accurate method is to measure the properties
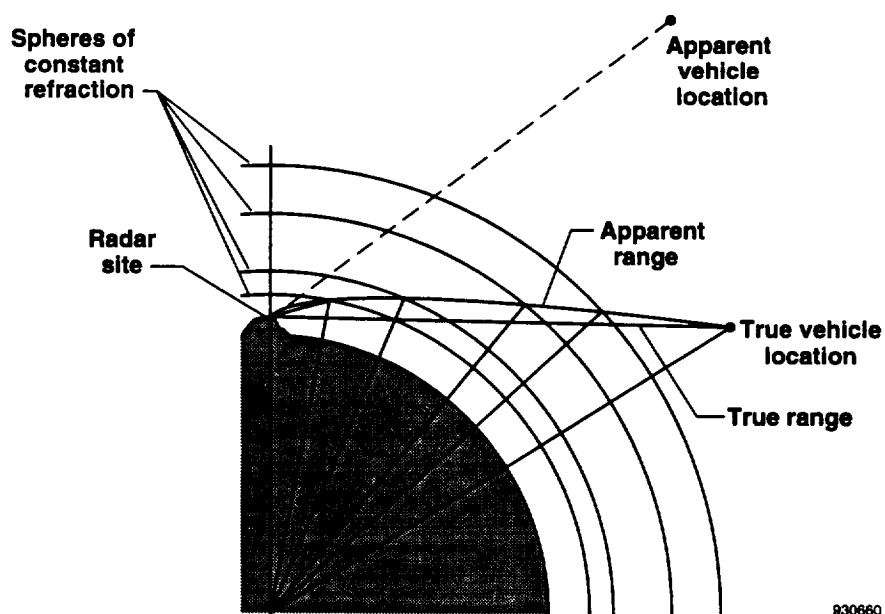

Figure 1. Effect of a nonhomogeneous atmosphere on a radar beam.

using a single weather balloon. The most nearly accurate method is to use all available weather data after the flight to generate a model of the atmosphere for the time of flight of the vehicle.[1] This method takes considerable effort. The first two methods may be used in real time, but the third method must be used after the flight. When the highest degree of accuracy is desired, the third method is used.

Figure 2 shows a postflight-analyzed refractivity profile along with a profile extrapolated from surface conditions. The differences between the two models are significant for all but the shortest radar ranges.

This computer program provides two methods of correcting for atmospheric refraction errors. The first is called the gradient refraction method,[4] which analyzes the radar beam one short segment at a time to determine the incremental bending between segments. This method is the most nearly accurate. On the other hand, because many small segments are analyzed at each time point, the method is computationally slow. The second method is called the White Sands method because it was developed at White Sands Missile Range, New Mexico.[3] This method uses an empirical fit to *exact* refraction corrections, such as gradient refraction results, at a given radar site. As a result, the coefficients used are geographically specific. The White Sands method is a function of radar site atmospheric parameters, so the structure of the atmosphere above the radar site is assumed. This assumption contributes the greatest error to the method. As an advantage, this method is computationally fast.

Appendix C contains the derivations for index of refraction, gradient refraction, and White Sands methods and three improvements to the algorithms used in previous versions of "radar". The first improvement deals with the algorithm for computing scale height. In turn, scale height is used to extrapolate index of refraction above the radar site. The algorithm used in years past induces as much as a 10-percent error in the atmospheric refraction corrections.[5] Appendix C also contains an alternate method that is substantially more nearly accurate.[5]

The second improvement is a new truncation algorithm for the gradient refraction method. This algorithm substantially reduces computation time required yet retains the accuracy of the method. Figure 3 shows examples of the percentage savings realized by this truncation algorithm as a function of elevation angle for two ranges.

The third improvement deals with the White Sands method for Edwards AFB, California. The empirical constants used in years past for the White Sands method at NASA Dryden were inaccurate. New constants have been derived and are presented in appendix C. Figure 4 shows the error in vehicle position caused by elevation
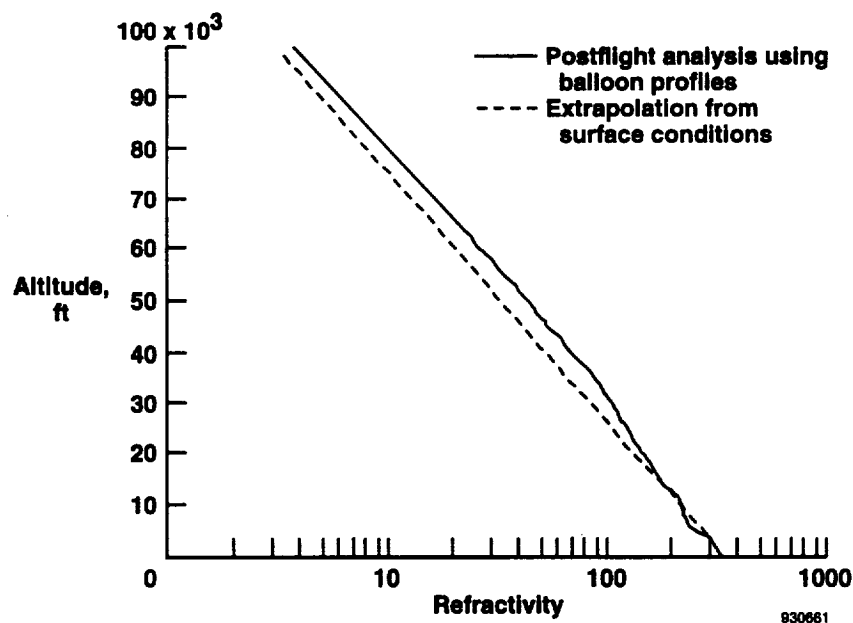
Figure 2. Refractivity profiles from postflight-analyzed balloon data and extrapolated surface conditions, Vandenberg AFB, California, April 5, 1990.
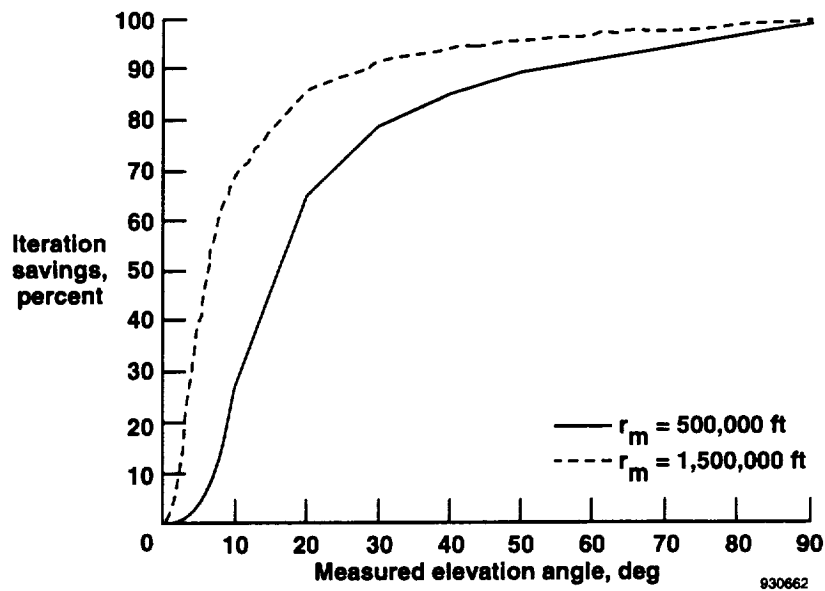
Figure 3. Truncation algorithm savings for radar 34 N_s = 338 and l_s = 500 ft.
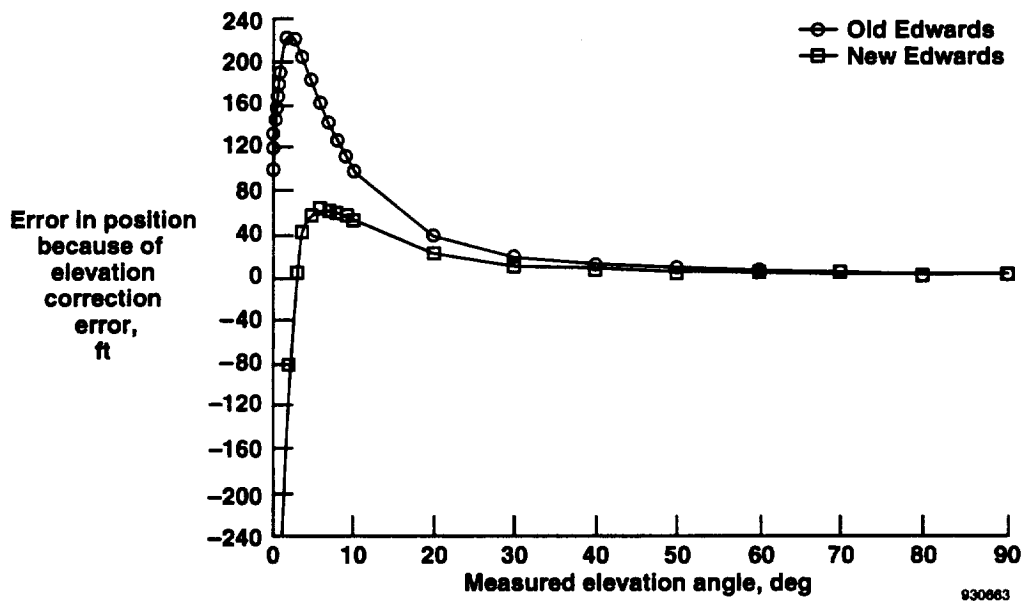
Figure 4. White Sands method errors in position as a result of an elevation correction error, where *zgeiod* = 2662.6 ft, r_m, = 600,000 ft, N_s = 338, and l_s = 500 ft. Here, the gradient refraction method is used as a truth model.

correction error as a function of measured elevation angle. Here, the gradient refraction method was used as the truth model. Most flight test work with radar data at NASA Dryden has been conducted at elevation angles above 10°. Refraction errors from using the White Sands method increase rapidly below this angle. Above 10°, using the new constants reduces the error in vehicle position by one-half as compared to using the old constants.

5

Spike Removal and Filtering

Spike removal and filtering of the raw range, azimuth, and elevation angle data are important options of this program. The spike removal routine detects spikes as large jumps in the derivative of the data and removes them by using a hold-last-rate scheme to estimate the true value of the data. The user selects if spike removal is to be performed and sets the criterion for spike detection.

Filtering of the raw data is performed with a discretized infinite impulse response (IIR) filter[6], which is a second-order, low-pass filter. The user selects the damping ratio and cutoff frequency of the filter. Appendix D provides a detailed description of the spike removal and filtering routines.

Velocity and Acceleration Determination

Once the position of the vehicle has been determined through geodetics, its velocity and acceleration can be calculated by taking derivatives. Such calculations are done by concatenating an open-loop zero with the IIR filter. The generation of noise associated with the taking of derivatives is suppressed by simultaneous low-pass filtering and differentiating. The user selects the cutoff frequencies for the velocity and acceleration filters. In addition, the user selects whether acceleration of gravity is subtracted from the vehicle acceleration. Acceleration of gravity is subtracted when radar acceleration is to be compared to acceleration from onboard accelerometers. Appendix D also gives the details of the velocity and acceleration calculations. When the cutoff frequency is selected to be zero, a second-order accurate, backwards difference differentiator is used instead of the IIR filter differentiator.[7]

Earth Relative and Airdata Parameters

The Earth relative parameters of total velocity, V, flightpath heading, Ψ, and flightpath angle, γ, are derived in appendix E. If atmospheric data as a function of altitude are input, then airdata parameters can be calculated. These airdata parameters consist of true airspeed, V_∞, true Mach number, M_∞, pressure altitude, H_p, ambient pressure, Ps_∞, and dynamic pressure, $\bar{q}$, and are also derived in appendix E. The atmospheric data needed are pressure altitude, ambient temperature, windspeed, wind direction, and lateral pressure gradient magnitude and direction. Appendix F gives the form of the atmospheric data.

PROGRAM USE

Appendix F contains specific instructions for running the program on the SUN 600 computer (Sun Microsystems, Incorporated, Mountainview, California), including all input and output files and parameters.

METHOD LIMITATIONS

This section describes the limitations and expected errors of the "radar" program. The primary limitation involves memory. Errors of note include refraction correction, spike removal, filtering, and differentiation.

Memory

The refraction and atmospheric tables can each accommodate a maximum of 100 altitude breakpoints. The size of arrays for filtering and differentiation is 75,000, allowing at least 60 min of 20-sample/sec data to be analyzed in one run of the "radar" program. These array sizes can only be changed in the source code.

Refraction Correction Errors

Because the true position of the vehicle is unknown, determining the errors due to refraction corrections is difficult. Several potential sources of errors in computing the refraction corrections exist. First, the value for refractivity at the radar site may have errors because of temperature and pressure measurement errors. Above the radar site, the relationship of refractivity with altitude may be assumed to be decaying exponentially. The result of such an assumption can be quite different from the true profile as shown by figure 2. If a profile of refractivity with altitude is determined by a weather balloon, balloon measurement errors will add to the refraction correction errors. Both of these profiles are assumed to be constant horizontally and in time. Again, such an assumption can be erroneous.

The gradient refraction method is regarded as the most accurate method for calculating refraction corrections. Accuracy of this method depends on the length of the segment, and its optimum value depends on the roundoff and truncation errors of the computer. The accuracy of the refraction profile of the atmosphere also affects the accuracy of the gradient refraction method. Generally, one or two least significant bits (LSB) of angle error may remain after gradient refraction corrections are applied. The magnitude of the error depends on the quality of the refractivity profile. For the AN/FPS-16 radars at Edwards AFB, California, one LSB is approximately 0.0027°. There are 17 bits in a 360° circle. The White Sands method is an approximation to the gradient refraction method. Figure 4 shows typical differences between the two methods.

Spike Removal, Filters, and Differentiation

The spike removal routine needs to have spike-free data for the first few data points. In addition, depending on the value of a user-defined rejection criterion, some spikes may remain in the data, or some good data which are somewhat erratic may have been removed. The user should always run the program with the spike remover option turned off and compare those results to the results of running the program with the spike remover turned on. The low-pass IIR filter tends to smooth out jumps in the data that may be real, such as an acceleration jump of an air-launched vehicle. Even though the time lag induced by the filtering is removed by time shifting the filtered parameters, some phase shifting of these data remains at the higher frequencies. These filters have start-up transients, especially when taking derivatives, and this fact should be considered when choosing data start times.

Other Expected Errors

The variability of the geoid separation with geography induces errors in the altitude above mean sea level. A bias may be applied to take into account the difference in geoid separation from the radar site to another location, but this approach does not totally address the problem.

Table 2 lists typical errors in data from the NASA Dryden AN/FPS-16 radars.[8] Note that these estimates represent the errors that would be present if no corrections were made, except for the best possible manual alignments. Some of these errors are considerably less than those given for other installations because rigorous calibrations and maintenance are performed routinely at this installation. From this table and the discussion in the Refraction Correction Errors subsection, mislevel, solar heating, and refraction correction errors are the largest errors in the radar data. Mislevel readings are taken periodically and are kept within specifications, currently 10 arc sec. This program allows for finer correction to mislevel as well as makes refraction corrections, but other sources of errors are currently neglected.

Table 2. Typical estimated errors in the NASA Dryden AN/FPS-16 radar.[8]

Source	Type	Typical, mrad	Typical, ft	LSB values
Thermal, range	Noise	—	2.6	0.41
Thermal, angle	Noise	0.02	—	0.40
R-f axis shift	Bias	—	~0	—
Droop, *el*	Bias	0.03	—	0.61
Orthogonality	Bias	0.02	—	0.41
Mislevel	Bias	0.05	—	1.00
LSB precision	Noise	0.03	3.2	0.50
Solar heating	Bias	0.05	—	1.00
Wind force	Bias	0.01	—	0.20
Antenna unbalance	Bias	—	~0	—
Servo unbalance	Bias	0.01	—	0.20
Dynamic lag*	Bias	0.01	—	0.20
Glint*	Noise	0.00	—	0.00
Vertical deflection	Bias	0.02	—	0.40
Earth model	Bias	0.01	—	0.20

*Target at 150n. mi.

CONCLUDING REMARKS

A postflight FORTRAN program called "radar" that reads and analyzes ground-based radar data from any radar site has been presented. This program provides Earth relative position, velocity, and acceleration as well as airdata parameters if atmospheric characteristics are input. A general description of methods used, program use, input, output, and method limitations has been given. Detailed derivations of algorithms are given in the appendixes.

In addition to documenting algorithms that have been used in earlier versions of this program, this report presents several new techniques and refinements. These techniques and refinements include an improvement in speed to the exact solution for geodetic altitude, an improved algorithm for determining scale height, a truncation algorithm for speeding up the gradient refraction method, and a refinement of coefficients used in the White Sands method for Edwards AFB, California.

Dryden Flight Research Center
National Aeronautics and Space Administration
Edwards, California, May 28, 1993

APPENDIX A

GEODETICS DERIVATION

The Earth can be described as an ellipse of revolution with semimajor axis, a, semiminor axis, b, and axis of revolution through the North and South Poles (fig. A-1). Considering a slice of the Earth that contains the axis of revolution (fig. A-2), a circle of radius a can be constructed.
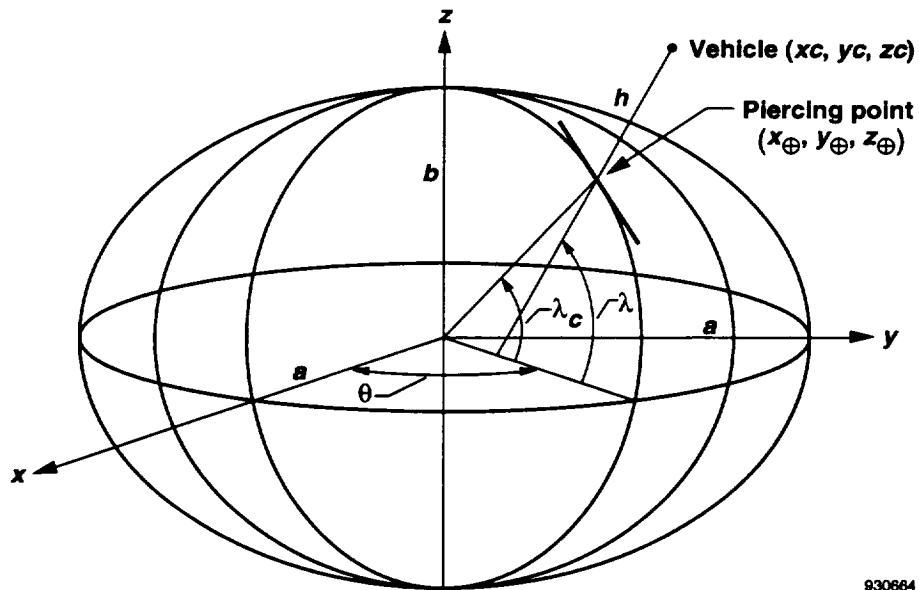
Figure A-1. Ellipsoid geometry.
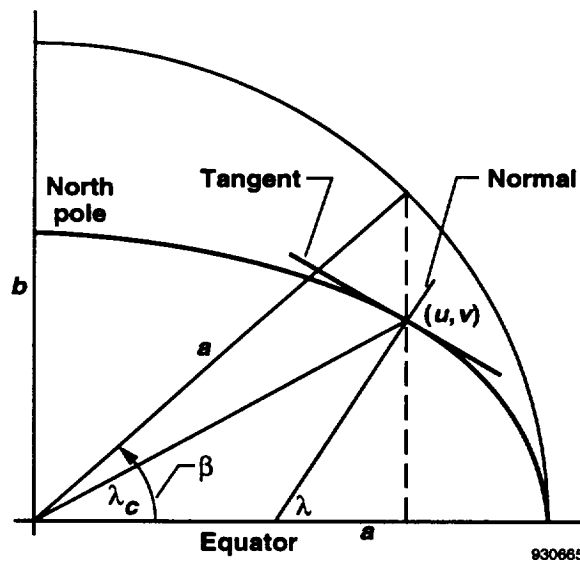
Figure A-2. Geodetic geometry for a point on the ellipsoid.

Three angles are associated with any given point on the surface of the Earth: λ_c, λ, and β. The geocentric latitude, λ_c, is the angle between (u, v), the center of the Earth, and the equitorial plane. The geodetic latitude, λ, is the latitude shown on maps and is the angle that the local vertical line through (u, v) makes with the equatorial plane. Figure A-2 shows the reduced latitude, β.[9] From this figure,

$$u = a\cos(\beta) \qquad \text{and} \qquad v = b\sin(\beta) \qquad \text{(A-1)}$$

To find the relationship between these three angles, the following equation of an ellipse is used:

$$\frac{u^2}{a^2} + \frac{v^2}{b^2} = 1 \qquad \text{(A-2)}$$

Differentiating implicitly and rearranging for the slope of the ellipse gives

$$\frac{dv}{du} = \frac{-b^2 u}{a^2 v} \qquad \text{(A-3)}$$

The local vertical to the ellipse has a slope of

$$-\frac{du}{dv} = \frac{a^2 v}{b^2 u} = \tan(\lambda) \qquad \text{(A-4)}$$

In addition from figure A-2,

$$\tan(\lambda_c) = \frac{v}{u} \qquad \text{(A-5)}$$

As a result,

$$\tan(\lambda) = \frac{a^2}{b^2} \tan(\lambda_c) \qquad \text{(A-6)}$$

Differentiating equation (A-1) gives

$$\frac{du}{dv} = \frac{-a}{b} \tan(\beta) \qquad \text{(A-7)}$$

10

Thus,

$$\tan(\lambda) = \frac{a}{b}\tan(\beta) = \left(\frac{a}{b}\right)^2 \tan(\lambda_c) \tag{A-8}$$

Having expressions for the sine and cosine of reduced latitude in terms of geodetic latitude will be useful later in this dicussion. Using equation (A-8) and the definition of the tangent gives

$$\tan(\beta) = \frac{\frac{b}{a}\sin(\lambda)}{\cos(\lambda)} = \frac{S}{C} \tag{A-9}$$

Solving for the sine and the cosine, while noting that the eccentricity, e, of the ellipse is by definition

$$e^2 = 1 - \left(\frac{b}{a}\right)^2 \tag{A-10}$$

which gives

$$\sin(\beta) = \frac{S}{\sqrt{S^2 + C^2}} = \frac{\frac{b}{a}\sin(\lambda)}{\sqrt{\left(\frac{b}{a}\right)^2 \sin^2(\lambda) + \cos^2(\lambda)}}$$

$$\tag{A-11}$$

$$= \frac{\frac{b}{a}\sin(\lambda)}{\sqrt{(1-e^2)\sin^2(\lambda) + \cos^2(\lambda)}} = \frac{\frac{b}{a}\sin(\lambda)}{\sqrt{1-e^2\sin^2(\lambda)}}$$

Similarly,

$$\cos(\beta) = \frac{C}{\sqrt{S^2 + C^2}} = \frac{\cos(\lambda)}{\sqrt{1-e^2\sin^2(\lambda)}} \tag{A-12}$$

The position of a radar site is generally given in terms of geodetic latitude, λ_s, longitude, θ_s, and height above the ellipsoid, h_s, where the s subscript denotes "of the radar site." From equation (A-1) and adding the increment for height, the position of the radar site in terms of u and v is

$$u_s = a\cos(\beta_s) + h_s\cos(\lambda_s) \tag{A-13}$$

$$v_s = b\sin(\beta_s) + h_s\sin(\lambda_s) \tag{A-14}$$

11

Getting the position of the radar site in terms of Cartesian geocentric coordinates, xc, yc, and zc is desired. The x axis lies in the equatorial plane and points towards the prime meridian (0° longitude), the z axis points towards the North Pole, and the y axis completes the right-handed system as shown in figure A-1. Because

$$xc = u\cos(\theta) \qquad \text{and} \qquad yc = u\sin(\theta) \qquad\qquad \text{(A-15)}$$

using equations (A-11) and (A-12), the Cartesian geocentric coordinates for the radar site are shown to be

$$xc_s = \left(\frac{a}{\sqrt{1 - e^2 \sin^2(\lambda_s)}} + h_s \right) \cos(\lambda_s)\cos(\theta_s) \qquad\qquad \text{(A-16)}$$

$$yc_s = \left(\frac{a}{\sqrt{1 - e^2 \sin^2(\lambda_s)}} + h_s \right) \cos(\lambda_s)\sin(\theta_s) \qquad\qquad \text{(A-17)}$$

$$zc_s = \left(\frac{a(1 - e^2)}{\sqrt{1 - e^2 \sin^2(\lambda_s)}} + h_s \right) \sin(\lambda_s) \qquad\qquad \text{(A-18)}$$

Now that the location of the radar site is known, the position of the vehicle with respect to the radar site can be added to this location to obtain the total vehicle position vector.

Consider a right-handed coordinate system centered at the radar antenna that points locally north, east, and down, x_l, y_l, and z_l. Assuming that the range, azimuth, and elevation have been corrected for various errors, the position of the vehicle is

$$x_l = r_r\cos(az)\cos(el_r)$$

$$y_l = r_r\sin(az)\cos(el_r) \qquad\qquad \text{(A-19)}$$

$$z_l = -r_r\sin(el_r)$$

12

These components are transformed into the geocentric coordinates by rotating them through latitude and longitude and adding the radar site position to get

$$
\begin{bmatrix} \cos(\theta_s) & -\sin(\theta_s) & 0 \\ \sin(\theta_s) & \cos(\theta_s) & 0 \\ 0 & 0 & 1 \end{bmatrix} \begin{bmatrix} \cos(-180° - \lambda_s) & 0 & \sin(-180° - \lambda_s) \\ 0 & 1 & 0 \\ -\sin(-180° - \lambda_s) & 0 & \cos(-180° - \lambda_s) \end{bmatrix} \begin{bmatrix} x_l \\ y_l \\ z_l \end{bmatrix} + \begin{bmatrix} xc_s \\ yc_s \\ zc_s \end{bmatrix}
$$

(A-20)

$$
= \begin{bmatrix} -\sin(\lambda_s)\cos(\theta_s) & -\sin(\theta_s) & -\cos(\lambda_s)\cos(\theta_s) \\ -\sin(\lambda_s)\sin(\theta_s) & \cos(\theta_s) & -\cos(\lambda_s)\sin(\theta_s) \\ \cos(\lambda_s) & 0 & -\sin(\lambda_s) \end{bmatrix} \begin{bmatrix} x_l \\ y_l \\ z_l \end{bmatrix} + \begin{bmatrix} xc_s \\ yc_s \\ zc_s \end{bmatrix} = \begin{bmatrix} xc \\ yc \\ zc \end{bmatrix}
$$

Now that the geocentric coordinates of the vehicle are known, the altitude of the vehicle above the ellipsoid can be determined (appendix B). Part of this process involves finding the point on the Earth directly below the vehicle, known as the piercing point, $x_\oplus$, $y_\oplus$, $z_\oplus$, (fig. A-1). Because equations (A-1) through (A-12) are only valid for a point on the surface of the ellipse, the piercing point must be used to determine vehicle latitude. Using equation (A-5), the geocentric latitude is

$$
\lambda_c = \tan^{-1}\left[\frac{z_\oplus}{\sqrt{x_\oplus^2 + y_\oplus^2}}\right]
$$

(A-21)

Geocentric latitude can be converted to geodetic latitude using equation (A-8)

$$
\lambda = \tan^{-1}\left[\left(\frac{a}{b}\right)^2 \tan(\lambda_c)\right]
$$

(A-22)

The longitude of the vehicle is determined by

$$
\theta = \tan^{-1}\left[\frac{yc}{xc}\right]
$$

(A-23)

Knowing the position of the piercing point relative to the radar site is often useful, such as when the ground track of the vehicle is desired. A difficulty arises on a nonflat Earth because traveling a certain distance north and then east will result in a different point than traveling first east than north, especially near the poles. For this reason, the distance from the radar site north to the latitude of the piercing point, xr, and the distance east from the radar site to the longitude of the piercing point, yr, is computed.

The distance xr can be determined by taking the arc length along the ellipse of the Earth, that is, along the radar site longitude, from the radar site to the piercing point latitude and substituting equations (A-1) and (A-10) to get

13

$$xr = \int_s^\oplus \sqrt{\left(\frac{du}{d\beta}\right)^2 + \left(\frac{dv}{d\beta}\right)^2} \, d\beta = \int_s^\oplus \sqrt{a^2 \sin^2(\beta) + b^2 \cos^2(\beta)} \, d\beta$$

$$\text{(A-24)}$$

$$= a \int_s^\oplus \sqrt{1 - e^2 \cos^2(\beta)} \, d\beta$$

which is an elliptical integral and must be calculated numerically. The "radar" program completes such calculations using Simpson's Rule. A linear interpolation is used to select the values for a given β, and the difference in values from the radar site and piercing point is xr.

The distance yr is the length of a circular arc from the vehicle longitude to the radar site longitude along the radar site latitude. From equations (A-1) and (A-12),

$$yr = u_s(\theta - \theta_s)\frac{\pi}{180°} = a\cos(\beta_s)(\theta - \theta_s)\frac{\pi}{180°} = \frac{a\cos(\lambda_s)}{\sqrt{1 - e^2 \sin^2(\lambda_s)}}(\theta - \theta_s)\frac{\pi}{180°} \qquad \text{(A-25)}$$

Another geodetic quantity required for appendix C is the local radius of curvature of the Earth at the radar site, Re. From the definition of radius of curvature,

$$Re = \frac{\left[1 + \left(\frac{du}{dv}\right)^2\right]^{1.5}}{\left|\frac{d^2u}{dv^2}\right|} \qquad \text{(A-26)}$$

Taking the derivative of equation (A-7) gives

$$\frac{d^2u}{dv^2} = \frac{d\left(-\frac{a}{b}\tan(\beta)\right)}{d\beta}\frac{d\beta}{dv} = \frac{-a}{b^2 \cos^3(\beta)} \qquad \text{(A-27)}$$

Substituting equations (A-7) and (A-27) into equation (A-26) gives

$$Re = \frac{\left\{1 + \left[\frac{a}{b}\tan(\beta)\right]^2\right\}^{1.5}}{\dfrac{a}{b^2 \cos^3(\beta)}} = \left\{\frac{a^2 \sin^2(\beta) + b^2 \cos^2(\beta)}{b^2 \cos^2(\beta)}\right\}^{1.5}\frac{b^2 \cos^3(\beta)}{a}$$

$$\text{(A-28)}$$

$$= \frac{\{a^2 \sin^2(\beta) + b^2 \cos^2(\beta)\}^{1.5}}{ab}$$

14

From the definition of sin(β) and cos(β) in equations (A-11) and (A-12), and noting that the radius of curvature at the radar site is required. That is,

$$Re = \frac{\left\{\dfrac{b^2 \sin^2(\lambda_s) + b^2 \cos^2(\lambda_s)}{1 - e^2 \sin^2(\lambda_s)}\right\}^{1.5}}{ab} = \frac{b^2}{a}\left\{1 - e^2 \sin^2(\lambda_s)\right\}^{-1.5} \tag{A-29}$$

APPENDIX B

ALTITUDE DERIVATION

An exact method for determining altitude above an ellipsoid is presented by Hedgley[10], and is outlined here with an improvement. In the original method, a fourth-order polynomial is solved. Each of the four roots must be used to determine four altitudes, and the lowest altitude is the correct answer. It is proven below that the minimum root is always the correct root. Because radar data are typically measured at 20 samples/sec and altitude is computed at every time point, this approach provides a substantial savings of computation time.

The distance from the vehicle to a point on the ellipsoid is given by

$$d = \sqrt{(x - xc)^2 + (y - yc)^2 + (z - zc)^2} \tag{B-1}$$

where (x, y, z) is a point on the ellipsoid, and (xc, yc, zc) is the vehicle point. Figure A-1 shows this geometry. The minimum distance is the altitude and is determined using the Lagrange multiplier method[11] where

$$J(x, y, z) = (x - xc)^2 + (y - yc)^2 + (z - zc)^2 - \alpha\left(\frac{x^2}{a^2} + \frac{y^2}{a^2} + \frac{z^2}{b^2} - 1\right) \tag{B-2}$$

Taking partial derivatives and equating them to zero gives

$$\frac{\partial J}{\partial x} = 2(x - xc) - \frac{\alpha 2x}{a^2} = 0 \qquad \text{or} \qquad x = \frac{xc\, a^2}{a^2 - \alpha} \tag{B-3}$$

$$\frac{\partial J}{\partial y} = 2(y - yc) - \frac{\alpha 2y}{a^2} = 0 \qquad \text{or} \qquad y = \frac{yc\, a^2}{a^2 - \alpha} \tag{B-4}$$

$$\frac{\partial J}{\partial z} = 2(z - zc) - \frac{\alpha 2z}{b^2} = 0 \qquad \text{or} \qquad z = \frac{zc\, b^2}{b^2 - \alpha} \tag{B-5}$$

$$\frac{\partial J}{\partial \alpha} = -\frac{x^2}{a^2} - \frac{y^2}{a^2} - \frac{z^2}{b^2} + 1 = 0 \tag{B-6}$$

Substituting equations (B-3) through (B-5) into equation (B-6) to eliminate x, y, z and collecting terms in α yields

$$\left[\frac{1}{a^2 b^2}\right]\alpha^4 - 2\left[\frac{1}{a^2} + \frac{1}{b^2}\right]\alpha^3 + \left[4 + \frac{a^2}{b^2} + \frac{b^2}{a^2} - \frac{xc^2}{b^2} - \frac{yc^2}{b^2} - \frac{zc^2}{a^2}\right]\alpha^2$$

$$\tag{B-7}$$

$$+ 2[xc^2 + yc^2 + zc^2 - a^2 - b^2]\alpha + [a^2 b^2 - xc^2 b^2 - yc^2 b^2 - zc^2 a^2] = 0$$

16

A typographical error exists in the coefficient for α^2 in Hedgley's paper.[10] Parameters a, b, xc, yc, and zc are all scaled to a to avoid using large numbers, then rescaled back once the altitude and piercing point have been determined. The original method uses each of the four possible real roots in turn to calculate altitude, and the four altitudes are compared to find the lowest altitude, which is the correct answer.

The improvement reported here shows that the minimum real root gives the correct altitude. Taking equation (B-3), noting that the point on the ellipse is the piercing point, and rearranging for α gives

$$\alpha = \frac{a^2(x_\oplus - xc)}{x_\oplus} \tag{B-8}$$

The vehicle and the point below it must be in the same hemisphere, so xc and $x_\oplus$ have the same sign. For positive altitude, the magnitude of xc is greater than the magnitude of $x_\oplus$. As a result, α must be negative for positive altitude. For negative altitude, the magnitude of $x_\oplus$ is greater than the magnitude of xc, so α must be positive. For zero altitude, α must be zero. Similar arguments hold using equations (B-4) and (B-5).

Determining if any negative roots of equation (B-7), exist will be helpful. By Descartes' rule of signs[12], the number of negative roots of $f(\alpha) = 0$ is equal to the number of positive roots of $f(-\alpha) = 0$, which is equal to the number of sign changes of the coefficients of $f(-\alpha)$ or that number reduced by a positive even number. In equation (B-7), normalize all variables by a, so a' equals one, b' is slightly less than one, and the sum of the squares of position components are nearly equal to the square of the distance from the center of the Earth, $R_o'^2$. With these assumptions, using $-\alpha$ in place of α to look at the signs of the coefficients gives

$$[+]a^4 + [+]a^3 + [\sim 6 - \quad \sim R_o'^2]a^2 + 2[\sim 2 - R_o'^2]a + [\sim 1 - \quad \sim R_o'^2] = 0 \tag{B-9}$$

For the case of $\sim 1 > \sim R_o'^2$ (which is negative altitude), the signs of equation (B-9) are all positive, so no sign changes. For this reason, no negative roots exist for negative altitude. In all other cases, only one sign will change, so only one negative root exists for positive altitude.

Because xc and $x_\oplus$ have the same sign, α must be less than a^2 from equation (B-3). From equation (B-5), α must be less than b^2. Because for Earth, b is less than a, α must be less than b^2. Now, substituting equations (B-3), (B-4), and (B-5) into equation (B-1) gives

$$d^2 = (xc + yc)^2\left[\frac{\alpha}{a^2 - \alpha}\right]^2 + zc^2\left[\frac{\alpha}{b^2 - \alpha}\right]^2 \tag{B-10}$$

Figure B-1 shows a graph of d^2 as a function of α. Note that this figure shows one negative root for positive altitude and no negative roots for negative altitude. To prove that the shape of these curves is correct, the derivative with respect to α is taken. That is,

$$\frac{d(d^2)}{d\alpha} = 2(xc + yc)^2\left(\frac{a^2}{(a^2 - \alpha)^2}\right)\left[\frac{\alpha}{a^2 - \alpha}\right] + 2zc^2\left(\frac{b^2}{(b^2 - \alpha)^2}\right)\left[\frac{\alpha}{b^2 - \alpha}\right] \tag{B-11}$$

17
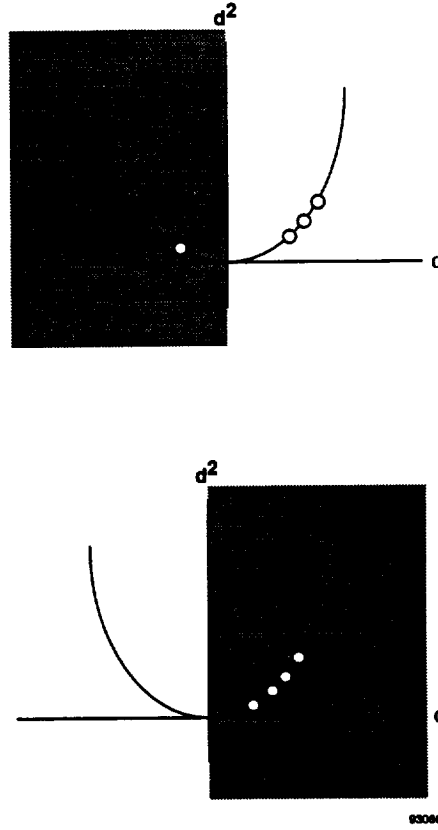
Figure B-1. Equation (B-10) roots as a function of Lagrange multiplier.

Only the terms in square brackets affect the sign of the derivative. For α positive, and noting that α is less than b^2, the derivative is positive. The larger α is, the bigger d^2 becomes. For α negative, the derivative is negative. Again, the larger the magnitude of α is, the bigger d^2 becomes. This fact is visualized by the concave upward shape of figure B-1. Because the root that gives the smallest value of d^2 is desired, the minimum positive real root or the maximum negative real root yields the true altitude.

For negative altitude, all the roots are positive. If the roots are all positive, then the minimum root yields the true altitude. For positive altitude, only one negative root exists, and the correct root must be negative. As a result, the minimum real root yields the true altitude; therefore in all cases, the minimum real root of equation (B-7) gives the correct value for altitude.

Now, determining the roots of a fourth-order polynomial is required. The solution to a quartic is given by Dickson[12] and is based on the work of Ferrari (1522–1565). Given quartic

$$x_q^{\ 4} + b_q x_q^{\ 3} + c_q x_q^{\ 2} + d_q x_q + e_q = 0 \qquad \text{(B-12)}$$

rearrange to get

$$x_q^{\ 4} + b_q x_q^{\ 3} = -c_q x_q^{\ 2} - d_q x_q - e_q \qquad \text{(B-13)}$$

18

Complete the square on the left-hand side

$$\left(x_q^2 + \frac{b_q}{2}x_q\right)^2 = \left(\frac{b_q^2}{4} - c_q\right)x_q^2 - d_q x_q - e_q \tag{B-14}$$

Adding

$$\left(x_q^2 + \frac{b_q}{2}x_q\right)y_c + \frac{y_c^2}{4} \tag{B-15}$$

to both sides gives

$$\left(x_q^2 + \frac{b_q}{2}x_q + \frac{y_c}{2}\right)^2 = \left(\frac{b_q^2}{4} - c_q + y_c\right)x_q^2 + \left(\frac{b_q y_c}{2} - d_q\right)x_q + \frac{y_c^2}{4} - e_q \tag{B-16}$$

and rearranging to get the resolvent cubic equation

$$y_c^3 - c_q y_c^2 + (b_q d_q - 4e_q)y_c - (b_q^2 e_q + 4c_q e_q - d_q^2) = 0$$

$$\tag{B-17}$$

$$= y_c^3 + b_c y_c^2 + c_c y_c + d_c$$

Now find any real root y_c of the resolvent cubic equation by setting

$$y_c = z_c - \frac{b_c}{3} \tag{B-18}$$

giving

$$z_c^3 + p z_c + q = 0 \tag{B-19}$$

which is the reduced cubic equation with

$$p = c_c - \frac{b_c^2}{3} \quad \text{and} \quad q = d_c - \frac{b_c c_c}{3} + \frac{2b_c^3}{27} \tag{B-20}$$

19

The discriminant of the reduced cubic and of the resolvent cubic is

$$\Delta = -4p^3 - 27q^2 \tag{B-21}$$

If $\Delta < 0$, then one root is real and two are complex. If $\Delta = 0$, then all the roots are real, and two or more are repeated. The real solution for $\Delta \leq 0$ is given by

$$z_c = \left(-\frac{q}{2} + \sqrt{\frac{\Delta}{-108}}\right)^{\frac{1}{3}} + \left(-\frac{q}{2} - \sqrt{\frac{\Delta}{-108}}\right)^{\frac{1}{3}} \tag{B-22}$$

If $\Delta > 0$, then three distinct real roots exist, and the following trigonometric solution is used:

$$\cos(3\angle) = 4\cos^3(\angle) - 3\cos(\angle) \tag{B-23}$$

Replacing $\angle$ by $\angle + 120°$ and $\angle + 240°$, in turn, gives

$$\cos(3\angle + 360°) = \cos(3\angle) = 4\cos^3(\angle + 120°) - 3\cos(\angle + 120°)$$

$$\cos(3\angle + 720°) = \cos(3\angle) = 4\cos^3(\angle + 240°) - 3\cos(\angle + 240°) \tag{B-24}$$

Thus, $\cos(\angle)$, $\cos(\angle + 120°)$, and $\cos(\angle + 240°)$ are the three roots of the equation

$$4t_c^3 - 3t_c = \cos(3\angle) \tag{B-25}$$

Hence,

$$t_c^3 - \frac{3}{4}t_c - \frac{\cos(3\angle)}{4} = 0 \tag{B-26}$$

To solve the reduced cubic equation, take $z_c = st_c$. The result is

$$t_c^3 + \frac{p}{s^2}t_c + \frac{q}{s^3} = 0 \tag{B-27}$$

20

with

$$s = \sqrt{\frac{-4p}{3}} \tag{B-28}$$

$$\cos(3\angle) = \frac{-q}{2}\left(\frac{-3}{p}\right)^{1.5} \tag{B-29}$$

As a result,

$$z_c = \sqrt{\frac{-4p}{3}} \cos\left\{\frac{\cos^{-1}\left[\frac{-q}{2}\left(\frac{-3}{p}\right)^{1.5}\right]}{3}\right\} \tag{B-30}$$

Now that z_c is known, a root of the resolvent cubic equation can be found. That is,

$$y_c = z_c - \frac{b_c}{3} \tag{B-31}$$

Returning to the quartic equation, the right-hand side of equation (B-16) is the square of a linear function. For example, $mx_q + n$. Thus,

$$\left(\frac{b_q^2}{4} - c_q + y_c\right)x_q^2 + \left(\frac{b_q y_c}{2} - d_q\right)x_q + \frac{y_c^2}{4} - e_q = a2x_q^2 + b2x_q + c2 = (mx_q + n)^2 \tag{B-32}$$

In addition,

$$x_q^2 + \frac{b_q}{2}x_q + \frac{y_c}{2} = mx_q + n$$

or

$$x_q^2 + \frac{b_q}{2}x_q + \frac{y_c}{2} = -mx_q + n \tag{B-33}$$

21

If $a2 = 0$, then the polynomial is a perfect square. The four roots to the quartic are the four roots of the following quadratics:

$$x_q^2 + \frac{b_q}{2}x_q + \frac{y_c}{2} - \sqrt{c2} = 0$$

(B-34)

$$x_q^2 + \frac{b_q}{2}x_q + \frac{y_c}{2} + \sqrt{c2} = 0$$

If $a2 \neq 0$, then the polynomial is not a perfect square. The four roots to the quartic are the four roots of the following quadratics:

$$x_q^2 + \left(\frac{b_q}{2} - m\right)x_q + \frac{y_c}{2} - n = 0$$

(B-35)

$$x_q^2 + \left(\frac{b_q}{2} - m\right)x_q + \frac{y_c}{2} + n = 0$$

where

$$m = \sqrt{a2}$$

(B-36)

$$n = \frac{b2}{2\sqrt{a2}}$$

When solving the two quadratic equations, the positive of the radical may be neglected because only the minimum roots are of interest. As a result, there will be one or two real roots from which to choose the minimum root.

Once the correct α is determined (the minimum α), the piercing point can be found by using equations (B-3), (B-4), and (B-5). The geocentric latitude, geodetic latitude, and longitude of the vehicle can be determined from equations (A-21), (A-22), and (A-23). Rearranging equations of the form of equations (A-16), (A-17), and (A-18) allows solving for the altitude of the vehicle by using one of the following three equations:

$$h' = \frac{xc'}{\cos(\lambda)\cos(\theta)} - \frac{a'}{\sqrt{1 - e^2 \sin^2(\lambda)}}$$

(B-37)

$$h' = \frac{yc'}{\cos(\lambda)\sin(\theta)} - \frac{a'}{\sqrt{1 - e^2 \sin^2(\lambda)}}$$

(B-38)

$$h' = \frac{zc'}{\sin(\lambda)} - \frac{a'(1 - e^2)}{\sqrt{1 - e^2 \sin^2(\lambda)}}$$

(B-39)

22

where

$$h = h'a \tag{B-40}$$

The proper equation is chosen to avoid division by values close to zero in the first term. These equations determine altitude with a higher computational accuracy than can be obtained by using equation (B-1). Lastly, because all parameters were scaled to a to avoid using large numbers, the altitude is scaled back by the value a.

APPENDIX C

REFRACTION CORRECTION DERIVATION

To calculate the amount of bending in the radar beam, the index of refraction of the atmosphere must be determined. The index of refraction is $\eta = 1.0$ in a vacuum, and $\eta > 1.0$ in the atmosphere. This index decreases with altitude in most cases. When dealing with air, it is useful to deal with refractivity, N, where

$$N = (\eta - 1)10^6 \qquad (C-1)$$

The refractivity ranges from 0 in space to the order of 300 at the ground; therefore, η ranges from 1.000000 to ~ 1.000300. The index of refraction at the radar site can be determined from site pressure and temperature measurements. Above this site, the index of refraction can be extrapolated or measured using weather balloons.

Refractivity at the radar site, N_s, is determined using the dry and wet bulb temperatures (°R), T_s and $Twet_s$, and the ambient pressure (in. Hg.), p_s, at the site by[13]

$$N_s = \frac{4730.3 p_s}{T_s} - \frac{341.36 ev}{T_s} + \frac{4.1146 \times 10^7 ev}{T_s^2} \qquad (C-2)$$

where[14]

$$ev = Twet_s{}^a 10^{\left[c + \frac{b}{Twet_s}\right]} - [f + g(Twet_s - d)]p_s(T_s - Twet_s) \qquad (C-3)$$

$$es = T_s{}^a 10^{\left[c + \frac{b}{T_s}\right]} \qquad (C-4)$$

Table C-1 gives constants a through g. The relative humidity given by

$$rh = \frac{ev}{es} \times 100 \qquad (C-5)$$

Table C-1. Constants for equations (C- 3) and (C-4).[14]

Constant	$Twet_s$ above freezing	$Twet_s$ below freezing
a	−4.9283	−0.32286
b	−5287.32	−4869.38
c	23.2801	10.0343
d	459.4	459.4
f	3.595×10^{-4}	3.595×10^{-4}
g	2.336×10^{-7}	2.336×10^{-7}

is checked to ensure that these pressures and temperatures do not yield values above 100 percent. Equation (C-2) is valid to within 0.5 percent for temperatures from -58 to 104 °F, pressures from 5.91 to 32.48 in. Hg., ev from 0 to 0.88 in. Hg., and radar frequencies up to 30,000 MHz.[13]

One way of determining refractivity at higher altitudes is to assume that it decays exponentially with geoid altitude. That is,

$$N = N_s e^{\left[\frac{h_s - gs_s - ze}{H\frac{3937ft}{1200m}}\right]} \tag{C-6}$$

where h_s is the ellipsoid altitude of the radar site, gs_s is the geoid separation at the radar site, ze is the ellipsoid altitude of interest, and H is the scale height.

Scale height can be assumed by iterating a function of N_s, using h_s to determine function coefficients.[5] The coefficients of this function were determined from a least squares fit of refraction correction data from nine tracking sites located throughout the world. The scheme uses an initial estimate of $H = 7000m$ and then iterates the equation

$$H = A - BN_s e^{\left[\frac{(h_s - gs_s)\frac{1200m}{3937ft} - C}{H}\right]} \tag{C-7}$$

until H converges where the coefficients A, B, and C are given in table C-2.[5] The program defines convergence as within 1 ft. This method is superior to the one previously used at NASA Dryden.[4, 15] The former method can cause errors in excess of 10 percent in radar refraction corrections for such semiarid areas as Edwards AFB, California.[5]

Another approach to determining refractivity at higher altitudes is to take a profile of refractivity as a function of altitude as measured by weather balloons. This approach is especially appropriate when the atmosphere has a high degree of nonexponentiality, such as when an inversion layer is present near the surface where most of the radar beam bending takes place. When interpolating between data points, altitude is interpolated linearly, and N is interpolated exponentially. The "radar" program extrapolates using the nearest two points for altitudes above and below the profile, so the end points should exhibit the same trend as the rest of the data.

This model of atmosphere refractivity is static, but the "radar" program could be modified to accept a time history of refractivity to do dynamic atmospheric refraction corrections. To date, no attempt has been made to take into account horizontal gradients of refractivity of the atmosphere. This effect may become significant during atmospherically active days, but those days would hopefully see little flight activity. With these caveats, refractivity can be determined for any altitude; now, a determination of how it affects the radar beam can be made.

Table C-2. Constants for equation (C-7).

Constant	$h_s < 1000$ m	1000 m $\le h_s < 2500$ m	$h_s \ge 2500$ m
A, m	17590.00	18588.000	21273.000
B, m	30.55	40.814	60.227
C, m	0.00	1500.000	3000.000

GRADIENT REFRACTION METHOD

For the gradient refraction correction, the time the radar beam takes to travel from the radar to the target is divided into a number of equal parts, *delt* being the time interval, and ns being the number of segments. It is assumed that the radar beam travels in a straight line during each time interval and has a discrete angular change between adjoining segments. The first segment leaves the radar at the measured elevation angle (fig. 1). Now assume that each segment consists of three beams (fig. C-1). The time interval in which the three beams travel is the same. Because the index of refraction, and thereby the speed of light, changes with altitude, the top beam travels the farthest, and the lower beam travels the least distance. As a result, the wave front becomes increasingly vertical, and the width of the beam increases.

Now, consider two adjoining segment triplets to see how the turning is calculated. The *n*th triplet is some distance from the radar site, and the local vertical there is tilted by the internal Earth angle, ia_n, from the radar site vertical. The beams Us_n, Ms_n, and Ls_n are at an elevation $el_n + ia_n$ to the local horizontal. Beam Ms_n starts at an altitude of h_n. Next estimate the ellipsoid altitude of the midpoint of beam Ms_n as

$$ze_n = h_n + \frac{c_o}{\eta_{n-1}} delt \frac{\sin(el_n + ia_n)}{2} \tag{C-8}$$

where c_o is the speed of light in a vacuum, and η_{n-1} is the index of refraction from the previous segment. Now, the refractivity at altitude ze_n, N_n, can be determined either through table lookup of balloon data or through equation (C-6).

The derivative of refractivity with respect to altitude, $\frac{\partial N}{\partial h}$, can be determined by differentiating Equation (C-6). That is,

$$\left(\frac{\partial N}{\partial h}\right)_n = -\frac{N_n}{H \frac{3937 ft}{1200 m}} \tag{C-9}$$
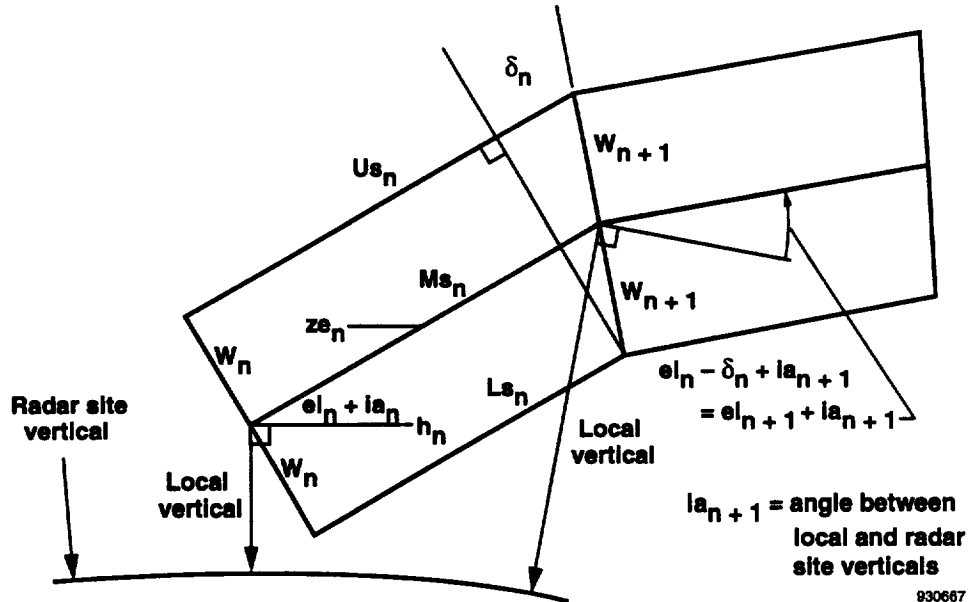
Figure C-1. Gradient refraction segment geometry.

where H is determined by equation (C-7) or by adjacent points in the balloon data. In the case of balloon data, H may differ for each segment. The index of refraction for the upper and lower beams is now

$$N_{n_u} = N_n + \left(\frac{\partial N}{\partial h}\right)_n w_n \cos(el_n + ia_n) \qquad \text{(C-10)}$$

$$N_{n_l} = N_n - \left(\frac{\partial N}{\partial h}\right)_n w_n \cos(el_n + ia_n) \qquad \text{(C-11)}$$

where w_n is the distance between the midbeam and the upper or lower beam of the current segment.
The lengths of the three beams are as follows:

$$Us_n = \frac{c_o}{\eta_{n_u}} delt \qquad \text{(C-12)}$$

$$Ms_n = \frac{c_o}{\eta_n} delt \qquad \text{(C-13)}$$

$$Ls_n = \frac{c_o}{\eta_{n_l}} delt \qquad \text{(C-14)}$$

The width of the next segment is

$$w_{n+1} = \sqrt{w_n^2 + \left(\frac{Us_n - Ls_n}{2}\right)^2} \qquad \text{(C-15)}$$

The turning angle is

$$\delta_n = \sin^{-1}\left(\frac{Us_n - Ls_n}{2w_{n+1}}\right) \qquad \text{(C-16)}$$

A plane tangent to the radar site can be defined, where D is the distance downrange of the radar site, and Z is the altitude above the tangent plane. The increment to tangent plane altitude and downrange because of this segment can be calculated in feet by

$$D_{n+1} = D_n + Ms_n \cos(el_n) \qquad \text{(C-17)}$$

$$Z_{n+1} = Z_n + Ms_n \sin(el_n) \qquad \text{(C-18)}$$

27

Note that the angle *ia* is not used in equations (C-17) and (C-18) because a radar site origin is being used instead of one local to the segment. The tangent plane position can be converted to altitude about a spherical Earth using the law of cosines and figure C-2.

$$h_{n+1} = \sqrt{(Re + h_s + Z_{n+1})^2 + D_{n+1}^2} - Re \tag{C-19}$$

To use equation (C-19), the radius of the Earth at the radar site, *Re*, is needed. Because the Earth is modeled as an ellipsoid, the local radius of curvature of the ellipse will be used. This radius is given by equation (A-29). The radius of curvature only needs to be computed once outside the refraction calculation loop because this radius only depends on radar site geodetic latitude and Earth characteristics. As an alternative to equation (C-19), the exact calculation for altitude given in appendix B may be used although this calculation greatly increases the amount of computation time required.

Next, the internal Earth angle, *ia*, is calculated. For the spherical Earth, this angle is obtained by the definition of the sine

$$ia_{n+1} = \sin^{-1}\left(\frac{D_{n+1}}{h_{n+1} + Re}\right) \tag{C-20}$$

For the ellipsoid, the definition of the dot product is used. The two vectors are the site vertical vector, s, and the local vertical vector, v. Both vectors are normal to their respective surfaces of the Earth; therefore,

$$ia_{n+1} = \cos^{-1}\left(\frac{s_1 v_{n+1_1} + s_2 v_{n+1_2} + s_3 v_{n+1_3}}{|s||v_{n+1}|}\right) \tag{C-21}$$
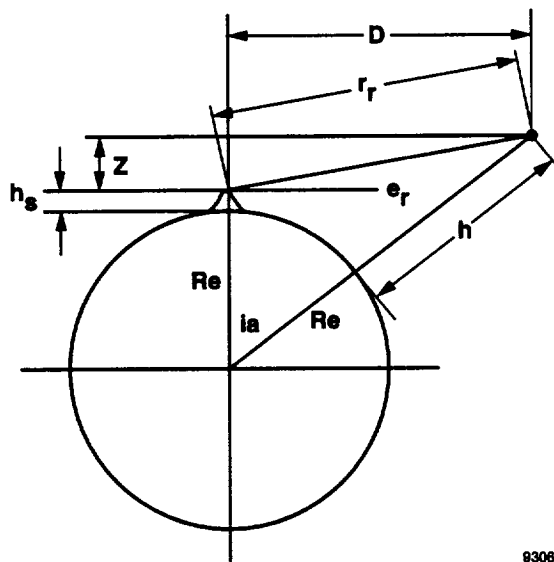
930668

Figure C-2. Gradient refraction method geometry for a spherical Earth.

28

Once, the parameters have been calculated for a single segment, the process is repeated for the subsequent segments with equations (C-8) through (C-19) and either (C-20) or (C-21) until all the segments have been analyzed. Referring back to figure C-2, the corrected range and elevation are determined by

$$r_r = \sqrt{D_{ns}^2 + Z_{ns}^2}$$

(C-22)

$$el_r = \tan^{-1}\left(\frac{Z_{ns}}{D_{ns}}\right)$$

(C-23)

The accuracy of the gradient refraction method depends on the length of the time segment, *delt*, and its optimum value depends on the roundoff and truncation errors of the computer. For the SUN 600 computer at NASA Dryden, a value of *delt* that gives 1000-ft segments in a vacuum is generally used. Although this value may not be the optimum, it was selected because data from balloon profiles of refractivity are received in 1000-ft intervals.

Because the largest gradient of refractivity with altitude occurs near the Earth, most of the bending of the radar beam occurs near the Earth. Above a certain altitude, the remaining turning in the radar beam may be insignificant. If the algorithm can be truncated above this point, a substantial computational savings is possible. An original method is presented now to determine when the gradient refraction algorithm may be truncated without introducing significant errors.

The turning angle decreases with increasing altitude. This decrease is assumed to be at the same rate as refractivity; therefore, the approximated turning angle is

$$\delta_n'' = \delta_n e^{\left[H\frac{-\Delta h_n}{\frac{3937 ft}{1200 m}}\right]}$$

(C-24)

where Δh_n is an estimate of the altitude of the target above the current segment

$$\Delta h_n = (ns - n + 1)Ms_n \sin(el_n + ia_n)$$

(C-25)

The difference between the free-space segment length and the segment length at a given altitude is likewise approximated as

$$(c_o delt - Ms_n)'' = (c_o delt - Ms_n)e^{\left[H\frac{-\Delta h_n}{\frac{3937 ft}{1200 m}}\right]}$$

(C-26)

29

The average turning that remains for each segment and the average segment length can be found by integrating with respect to altitude and dividing by the remaining altitude

$$\bar{\delta}_{n_{rem}} = \frac{\int_{h_n}^{h_{ns}} \delta'' dh}{\Delta h_n} = \frac{\int_{h_n}^{h_{ns}} \delta_n e^{\left[\frac{h_n - h}{H\frac{3937ft}{1200m}}\right]} dh}{\Delta h_n} = \frac{H\frac{3937ft}{1200m}\delta_n}{\Delta h_n}\left(1 - e^{\left[\frac{-\Delta h_n}{H\frac{3937ft}{1200m}}\right]}\right) \qquad (C\text{-}27)$$

$$\bar{M}_n = \frac{\int_{h_n}^{h_{ns}}\left[c_o delt - (c_o delt - Ms_n)''\right] dh}{\Delta h_n}$$

$$= c_o delt - \frac{H\frac{3937ft}{1200m}(c_o delt - Ms_n)}{\Delta h_n}\left(1 - e^{\left[\frac{-\Delta h_n}{H\frac{3937ft}{1200m}}\right]}\right) \qquad (C\text{-}28)$$

The remaining turning is the average turning multiplied by the number of remaining segments

$$\delta_{n_{rem}} = \bar{\delta}_{n_{rem}}(ns - n + 1) = \frac{H\frac{3937ft}{1200m}\delta_n(ns - n + 1)}{\Delta h_n}\left(1 - e^{\left[\frac{-\Delta h_n}{H\frac{3937ft}{1200m}}\right]}\right) \qquad (C\text{-}29)$$

The algorithm ends if the remaining turning is less than the minimum turning. Minimum turning is arbitrarily defined as 40 percent of the least significant bit of elevation. Because the digitization of elevation is 17 bits in a circle, the minimum turning is

$$\delta_{min} = 0.4\frac{360°}{2^{17}} \qquad (C\text{-}30)$$

If the algorithm is truncated early, the downrange distance from the radar site, D, and the altitude above the tangent plane, Z, need to be adjusted for the remaining segments. This adjustment is done by adding the components of the average segment length times the number of remaining segments. That is,

$$D_{ns} = D_n + \bar{M}_n(ns - n + 1)\cos(el_n) \qquad (C\text{-}31)$$

$$Z_{ns} = Z_n + \bar{M}_n(ns - n + 1)\sin(el_n) \qquad (C\text{-}32)$$

When inversion layers and other atmospheric phenomena are present near the ground, the index of refraction does not decay exponentially. Lack of such exponential decay can invalidate equations (C-24) and (C-26). For this reason, the gradient refraction algorithm does not truncate below a certain critical altitude where these conditions might exist. The radar program defaults to a critical geoid altitude of 10,000 ft; however, the user may select a different value. Figure 3 shows examples of the percentage of savings realized by this truncation algorithm as a function of elevation angle for two ranges.

WHITE SANDS METHOD

The White Sands method for refraction correction was created out of a need to process radar data easily and in nearly real time.[3] This method uses an empirical fit to *exact* refraction corrections, such as results of the gradient refraction methods at a given radar site. For this reason, the coefficients used are geographically specific. Because only radar site atmospheric conditions are quickly available, the structure of the atmosphere above the radar site is assumed. This assumption contributes the greatest error to the method. The method was designed to provide accurate results for elevation angles from 1° to 90° and for ranges of 500 to 200,000 yd.

A separate correction exists for elevation angle and range. Elevation angle correction will be discussed next. The refractivity at the radar site is used to calculate the constant K_{le}.

$$K_{le} = 10^{-6} \frac{6400}{2\pi} N_s \tag{C-33}$$

where there are 6400 army mils/2π radians. Then, the measured downrange and vertical distance from the radar site in yards, D and Z respectively, are calculated by

$$D = \frac{r_m}{3} \cos(el_m) \tag{C-34}$$

$$Z = \frac{r_m}{3} \sin(el_m) \tag{C-35}$$

These distances allow the elevation error in army mils to be calculated by

$$\Delta el = \frac{K_{le} D}{K_{2e} + Z} \tag{C-36}$$

where the constant K_{2e} will be discussed shortly. Lastly, the corrected elevation angle comes from

$$el_r = el_m - \frac{360°}{6400} \Delta el \tag{C-37}$$

31

Range is corrected in a similar manner by

$$\Delta r = \frac{K_{lr}D}{K_{2r} + Z}$$

(C-38)

so

$$r_r = r_m - 3\Delta r$$

(C-39)

The constants K_{2e}, K_{lr}, and K_{2r} are determined by a least squares fit of a large set of *exact* refraction corrections, over a range of values of el_m and r_m, for the desired radar site. These constants are a function of N_s. The constant K_{2e} is given by

$$K_{2e} = \frac{K_{le}\sum D\Delta el - \sum Z\Delta el^2}{\sum \Delta el^2}$$

(C-40)

The K_{lr} and K_{2r} are determined by the simultaneous linear equations (which are in error in reference 3)

$$K_{lr}\sum D^2 - K_{2r}\sum D\Delta r = \sum DZ\Delta r$$

(C-41)

$$K_{lr}\sum D\Delta r - K_{2r}\sum \Delta r^2 = \sum Z\Delta r^2$$

(C-42)

which transform to

$$K_{lr} = \frac{\left(\sum D\Delta r\right)\left(\sum Z\Delta r^2\right) - \left(\sum DZ\Delta r\right)\left(\sum \Delta r^2\right)}{\left(\sum D\Delta r\right)^2 - \left(\sum D^2\right)\left(\sum \Delta r^2\right)}$$

(C-43)

$$K_{2r} = \frac{\left(\sum D^2\right)\left(\sum Z\Delta r^2\right) - \left(\sum DZ\Delta r\right)\left(\sum D\Delta r\right)}{\left(\sum D\Delta r\right)^2 - \left(\sum D^2\right)\left(\sum \Delta r^2\right)}$$

(C-44)

Table C-3 shows values of these four constants for radars at Edwards AFB, California, and White Sands Missile Range, New Mexico.[3] The values labeled Old Edwards have been used at NASA Dryden for several decades; however, no documentation for them exists. Values for K_{lr} and K_{2r} did not exist for Edwards AFB, California, during that time. The values labeled New Edwards were computed using the gradient refraction algorithm with segment lengths of 500 ft; for ranges of 1,500, 3,000, 6,000, 15,000, 30,000, 60,000, 150,000, 300,000, and 600,000 ft; and for elevation angles of 2°, 5°, 12°, 25°, and 70°. These ranges and elevation angles are also used to

determine the White Sands constants. Computations using the New Edwards constants have approximately one half the error that the Old Edwards constants yield for elevation angles above 10° (fig. 4). The potential exists for optimizing the constants for a given radar coverage by selecting certain combinations of range and elevation angles, but this effort is left for future work.

Table C-3. Constants for equations (C-36) and (C-38).

N_s	K_{le}	Old Edwards K_{2e}, yd	New Edwards $zgeoid_s$ = 2662.593 ft			White Sands[3] $zgeoid_s$ = 4000 ft		
			K_{2e}, yd	K_{lr}, yd	K_{2r}, yd	K_{2e}, yd	K_{lr}, yd	K_{2r}, yd
220	0.2241	21410.6	19915.6	−3.627	15789.2	21790	−3.023	11980
222	0.2261	21160.5	19773.1	−3.630	15655.8			
224	0.2281	20916.6	19630.4	−3.633	15522.3	21200	−3.025	11820
226	0.2302	20679.8	19487.4	−3.636	15388.7			
228	0.2322	20449.3	19344.2	−3.638	15255.1	20650	−3.029	11680
230	0.2343	20224.7	19200.7	−3.639	15121.4			
232	0.2363	20005.9	19056.9	−3.640	14987.7	20130	−3.033	11540
234	0.2384	19792.9	18912.8	−3.640	14853.9			
236	0.2404	19585.2	18768.4	−3.640	14720.0	19610	−3.037	11400
238	0.2424	19382.8	18623.7	−3.639	14586.0			
240	0.2445	19185.4	18478.7	−3.638	14451.9	19110	−3.041	11270
242	0.2465	18993.0	18333.4	−3.636	14317.8			
244	0.2485	18804.8	18187.8	−3.634	14183.5	18650	−3.046	11140
246	0.2506	18621.5	18041.8	−3.631	14049.1			
248	0.2526	18442.3	17895.5	−3.627	13914.7	18250	−3.051	11020
250	0.2546	18267.3	17748.8	−3.623	13780.1			
252	0.2567	18096.4	17601.7	−3.618	13645.3	17900	−3.055	10890
254	0.2587	17929.1	17454.2	−3.613	13510.5			
256	0.2608	17765.9	17306.3	−3.607	13375.4	17550	−3.059	10760
258	0.2628	17606.1	17158.0	−3.601	13240.3			
260	0.2648	17449.7	17009.3	−3.594	13104.9	17200	−3.064	10640
262	0.2669	17296.8	16860.2	−3.586	12969.4			
264	0.2689	17147.1	16710.5	−3.578	12833.8	16870	−3.069	10520
266	0.2709	17000.6	16560.5	−3.569	12697.9			
268	0.2730	16857.2	16409.9	−3.560	12561.8	16550	−3.074	10400
270	0.2750	16716.7	16258.8	−3.550	12425.5			
272	0.2771	16579.0	16107.1	−3.539	12289.0	16250	−3.079	10280
274	0.2791	16444.2	15954.9	−3.528	12152.2			
276	0.2811	16312.0	15802.2	−3.517	12015.2	15970	−3.085	10170

Table C-3. Concluded.

		Old Edwards	New Edwards zgeoid$_s$ = 2662.593 ft			White Sands[3] zgeoid$_s$ = 4000 ft		
278	0.2832	16182.2	15648.8	−3.504	11877.9			
280	0.2852	16055.2	15494.8	−3.491	11740.3	15670	−3.090	10060
282	0.2872	15930.4	15340.2	−3.478	11602.4			
284	0.2893	15808.2	15184.9	−3.463	11464.2	15400	−3.095	9940
286	0.2913	15688.1	15028.9	−3.449	11325.7			
288	0.2934	15570.5	14872.1	−3.433	11186.8	15110	−3.100	9840
290	0.2954	15454.9	14714.6	−3.417	11047.5			
292	0.2974	15341.4	14556.3	−3.400	10907.7	14850	−3.105	9730
294	0.2995	15229.9	14397.2	−3.382	10767.6			
296	0.3015	15120.4	14237.2	−3.364	10627.0	14950	−3.111	9630
298	0.3035	15012.8	14076.3	−3.345	10485.9			
300	0.3056	14907.2	13914.4	−3.325	10344.3	14350	−3.117	9550
302	0.3076	14803.3	13751.4	−3.305	10202.1			
304	0.3097	14701.2	13587.5	−3.284	10059.3	14110	−3.122	9470
306	0.3117	14600.9	13422.4	−3.262	9915.9			
308	0.3137	14502.2	13255.8	−3.239	9771.6	13900	−3.128	9390
310	0.3158	14405.1	13089.1	−3.216	9627.5			
312	0.3178	14309.7	12919.7	−3.191	9481.5	13680	−3.135	9320
314	0.3198	14215.7	12749.5	−3.166	9335.1			
316	0.3219	14123.2	12577.0	−3.140	9187.2	13470	−3.141	9260
318	0.3239	14032.4	12403.5	−3.113	9038.7			
320	0.3259	13942.8	12228.1	−3.085	8889.2	13260	−3.148	9200
322	0.3280	13854.7	12051.0	−3.056	8738.5			
324	0.3300	13767.9	11871.8	−3.026	8586.5	13070	−3.155	9140
326	0.3321	13682.5	11689.8	−2.995	8432.6			
328	0.3341	13598.3	11505.9	−2.963	8277.6	12900	−3.162	9080
330	0.3361	13515.4	11319.6	−2.930	8121.0			
332	0.3382	13433.8	11130.4	−2.895	7962.6	12750	−3.169	9020
334	0.3402	13353.2	10938.2	−2.859	7802.1			
336	0.3422	13274.0	10741.9	−2.822	7638.8	12600	−3.177	8960
338	0.3443	13195.8	10542.4	−2.783	7473.4			
340	0.3463	13118.8	10338.8	−2.743	7305.2	12520	−3.184	8910

APPENDIX D

SPIKE REMOVAL, FILTERING, AND DIFFERENTIAL DERIVATION

The spike removal, filtering, and differentiation routines for the "radar" program are derived in this appendix. First, the spike detection and removal routines are described. Next, the transfer functions for the filtering and differentiation routines are presented. Then, the filters are discretized to give time recursive difference equations. Finally, the calculation of velocity and acceleration components is discussed.

SPIKE DETECTION AND REMOVAL

Automated spike detection and removal is an important utility of the program. Spike removal may be turned on or off. By default, such removal is not performed during the nominal code operation. The traditional difficulty with automated spike detection is in determining what constitutes a spike. Clearly, large data spikes can be detected and removed using such traditional statistical techniques as 3σ. Unfortunately, the 3σ technique will not reliably work for detecting subtle spikes which occur within the standard deviation of the data.

The spike detection and removal routines implemented in this program overcome this difficulty by differentiating the suspected spike-corrupted signal. Differentiating the signal greatly amplifies data spikes and renders them clearly distinguishable from the input data stream. This effect is illustrated in figure D-1 where a subtle spike in the input data stream is rendered extremely large in the differentiated signal. Clearly, if the original signal were used to perform the spike detection, the 3σ criterion would not have been violated. The spike would have remained undetected.
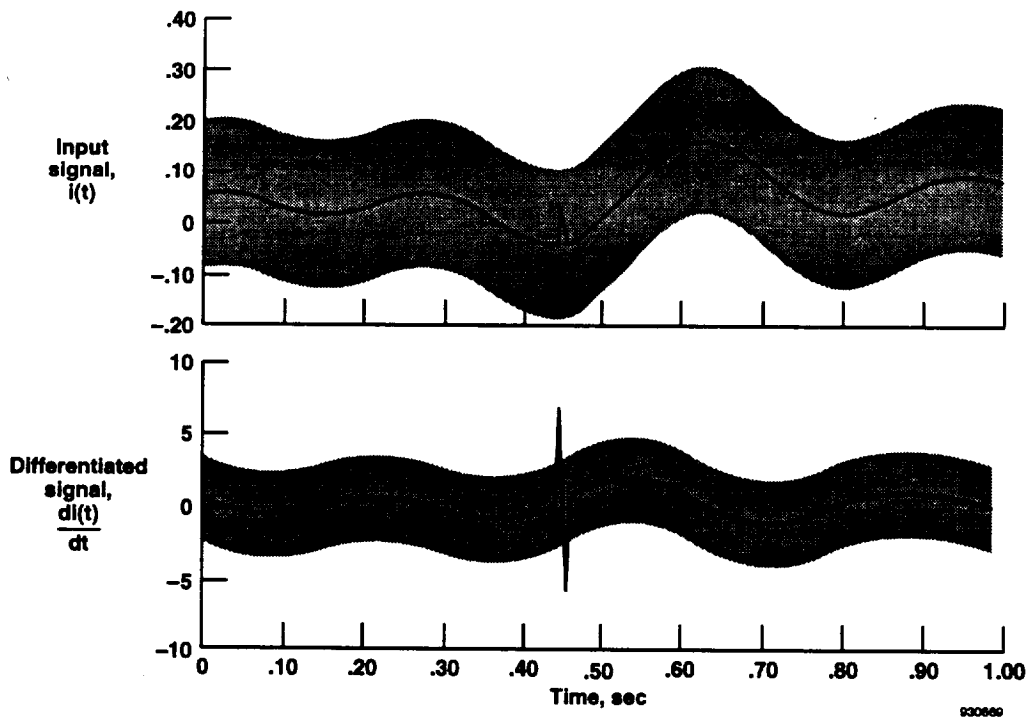

Figure D-1. Effect of differentiation of input data spike.

Conversely, the differentiated signal clearly violates the 3σ criterion at the data spike, and the data spike is easily detected. A sliding window, whose length is user defined, is used to accumulate sample mean and standard deviation statistics of the differentiated signal. The user also selects the number of standard deviations for the rejection criterion. When a data point is encountered whose magnitude deviation from the current sample mean exceeds the rejection criterion, then the point is rejected. The previous value of the derivative is used to extrapolate the original signal across the corrupted region. As such, the spike-editing routines perform a hold-last-rate interpolation. Mean and standard deviation statistics are calculated for a window twice: first using all derivative data, then again using derivative data that are within the criterion band. For spike detection, a first-order-accurate, backward-difference derivative is used. A single data spike will cause a large derivative at that point and another large derivative of opposite sign at the next point. As a result, two points will be removed. The filtered derivative described in the Differentiator Transfer Function subsection was not used. The effect of the one data spike would have been spread out over many data points because of the filtering. Hence, many data points would be removed.

The spike detection routine demands that the first few data points be spike free, and the last one-half window of data points will be discarded. The spike remover should never be used blindly on new data. First, run the data without using the spike remover to determine if it is needed. If so, use various numbers of standard deviations as the detection criterion, and inspect the results. A high number of standard deviations may allow many spikes to go undetected, and a low number may remove valid data points.

LOW–PASS FILTER TRANSFER FUNCTION

The filtering and differentiation routines for the program are based on the use of an infinite impulse response (IIR) filter to eliminate noise above a selected cutoff frequency.[6] In these routines, a second-order low-pass filter is used. The frequency domain transfer function of this filter is given by

$$\frac{O(s)}{I(s)} = \frac{1}{\left(\dfrac{s}{\omega_n}\right)^2 + 2\xi\left(\dfrac{s}{\omega_n}\right) + 1} \tag{D-1}$$

where ω_n is the natural resonance frequency, ξ is the damping ratio, and s is the Laplace transform variable. For sinusoidal inputs, $s = j\omega$, the magnitude and phase angle of the filter transfer function may be written as follows:

$$M(j\omega) = \frac{1}{\sqrt{\left[1 - \left(\dfrac{\omega}{\omega_n}\right)^2\right]^2 + \left[2\xi\left(\dfrac{\omega}{\omega_n}\right)\right]^2}} \tag{D-2}$$

In addition,

$$\phi(j\omega) = -\tan^{-1}\left\{\frac{2\xi\left(\dfrac{\omega}{\omega_n}\right)}{\left[1 - \left(\dfrac{\omega}{\omega_n}\right)^2\right]}\right\} \tag{D-3}$$

Figure D-2 shows a sample frequency response plot for a natural frequency of 0.5 Hz and several damping ratios.

With proper selection of the damping ratio, this transfer function allows the signal at low frequencies to be passed essentially unaltered. At the same time, the signal at frequencies beyond ω_n is attenuated greatly with a magnitude attenuation approaching 40 dB/frequency decade. Because equation (D-1) introduces a negative phase angle, it will have the effect of time-delaying the output signal. This lag is given by

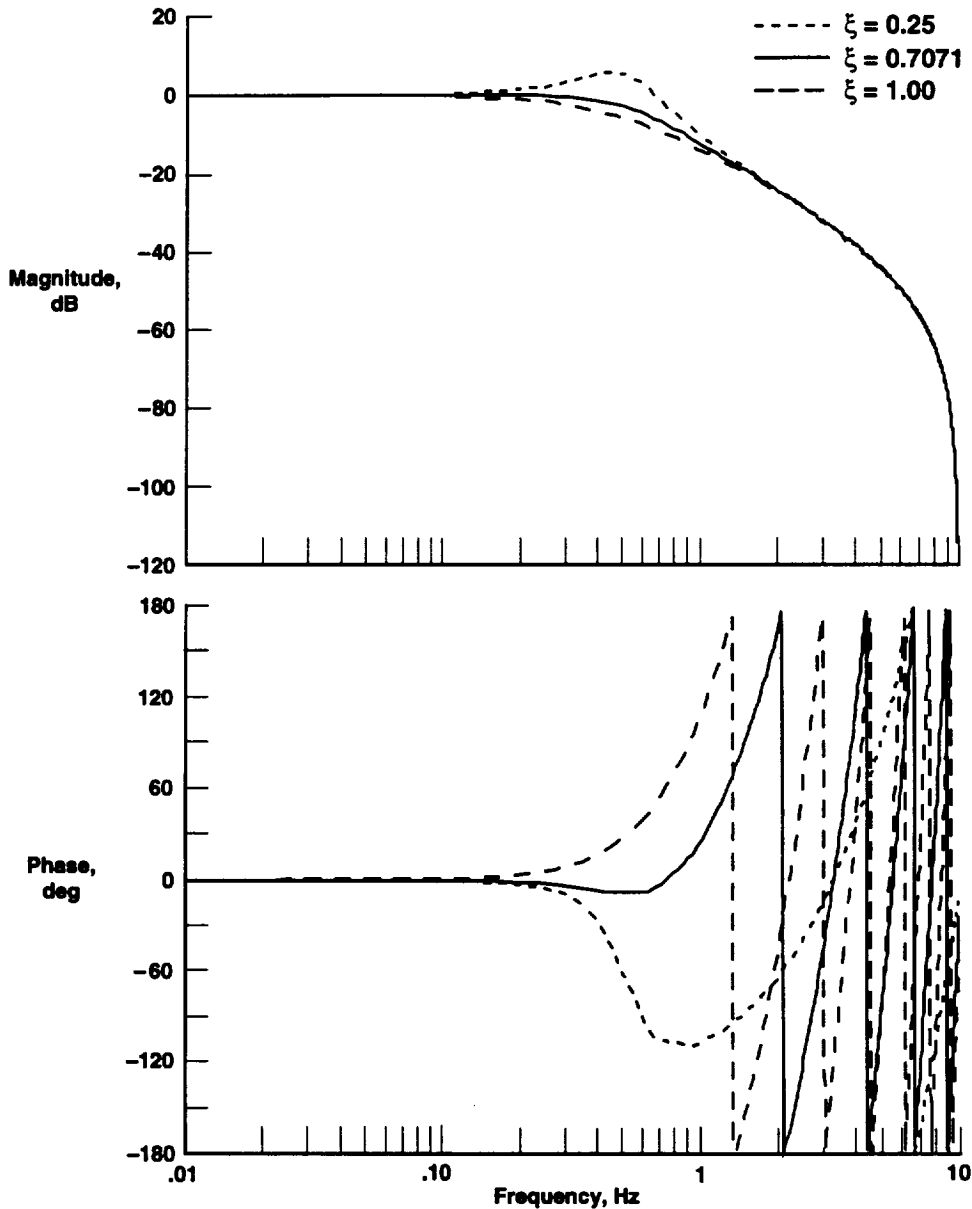$$\tau = \lim_{\omega \to 0} \frac{\phi(j\omega)}{\omega} = \frac{2\xi}{\omega_n} \qquad (D-4)$$

Figure D-2. Frequency response of low-pass infinite impulse response filter with time shifting for several damping ratios, $w_n = 0.5$ Hz.

37

Because filtered output signals are to be time-correlated with unfiltered input signals, this time delay is accounted for by after-the-fact time-shifting of all filtered signals. This time-shifting is taken into account in figure D-2 which shows nearly zero phase lag for frequencies less than ω_n.

DIFFERENTIATOR TRANSFER FUNCTION

The differentiator is derived from equation (D-1) by simply concatenating the filter transfer function with an open-loop zero (multiplying by s), which from Laplace transform mapping rules has the effect of differentiating the original signal. That is,

$$L\left[\frac{d}{dt}i(t)\right] = sI(s) - i(0) \tag{D-5}$$

The resulting transfer function is as follows:

$$\frac{O(s)}{I(s)} = \frac{s}{\left(\dfrac{s}{\omega_n}\right)^2 + 2\xi\left(\dfrac{s}{\omega_n}\right) + 1} \tag{D-6}$$

while using $i(0) = 0$. Because the open-loop zero tends to infinite magnitude at high frequency, it must be concatenated with the low-pass filter to attenuate high-frequency measurement noise. Failure to do so results in a differentiated signal that is overwhelmed by the overamplified noise.

Figure D-3 shows a sample frequency response plot for the differentiating filter at a natural frequency of 0.25 Hz and a damping ratio of 0.7071 with time-shifting. Notice that the magnitude appears to follow the proper slope through approximately 0.2 Hz. Beyond this frequency, the value rolls off, and the data no longer accurately represent the derivative. As a consequence, the derivative signal will always be reduced in frequency content from the original signal. As with the filtered data, a time delay occurs. This time delay is accounted for by after-the-fact time-shifting of all differentiated signals, as shown by the nearly flat 90° phase at the lower frequencies.

FILTER DISCRETIZATION

The frequency-domain transfer functions are for continuous-time signals. For application to discrete-time-sampled data signals, the filters must be mapped to the discrete-time Fourier plane, z-plane, and inverse transformed to give difference equations. These difference equations can be implemented recursively to process the input signals.

Mapping from the continuous-time frequency plane to the discrete-time Fourier plane is completed through the bilinear transform[6]. This mapping function is given by

$$s = \frac{2}{\Delta t}\left(\frac{z-1}{z+1}\right) \tag{D-7}$$

38
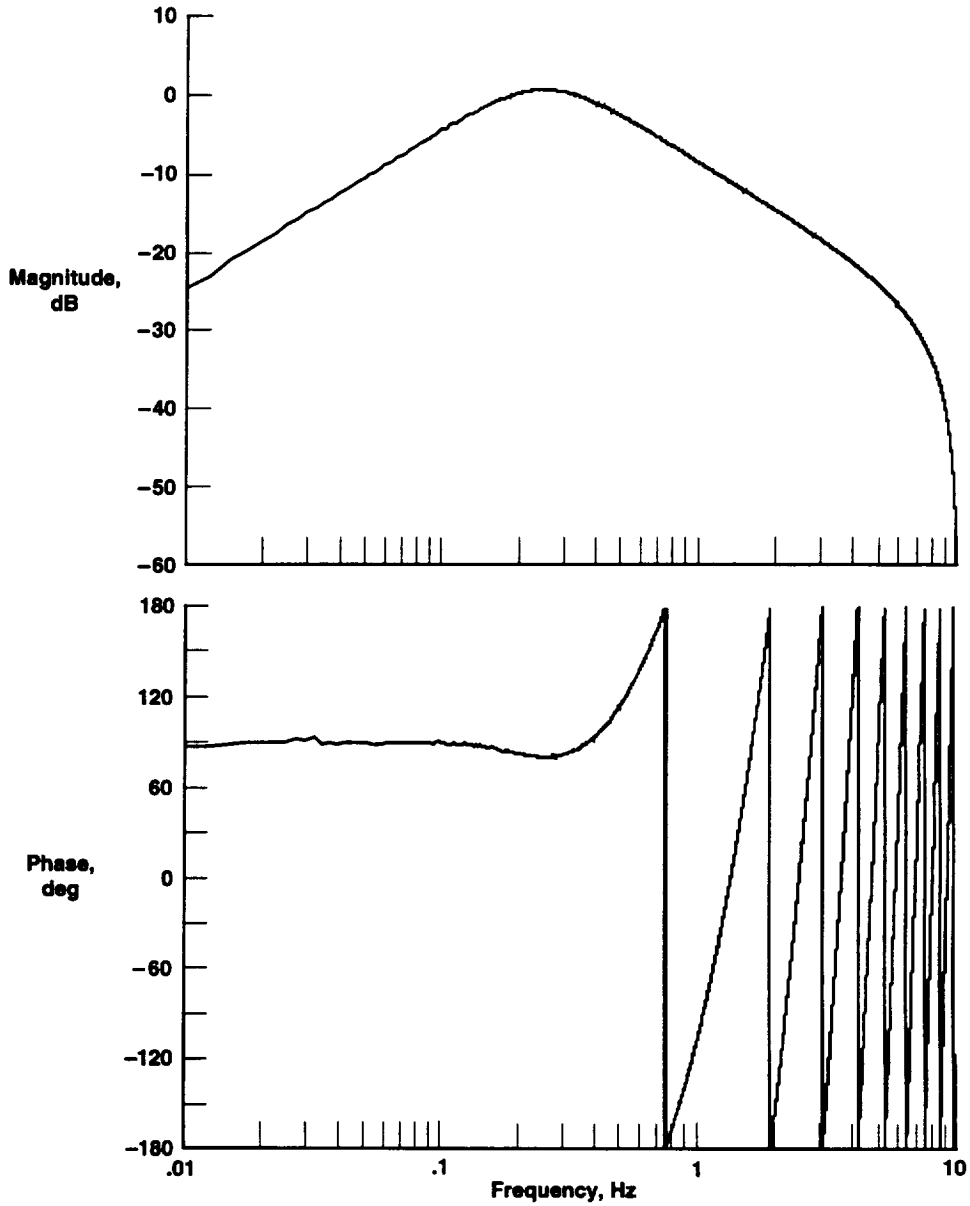
Figure D-3. Frequency response of low-pass infinite impulse response differentiator filter with time shifting, $w_n = 0.25$ Hz.

where Δt is the sample interval of the discrete-time system, and z is the discrete-time Fourier transform variable. If z is substituted into equation (D-1) and the results are collected, the resulting z-transform function for the low-pass filter is as follows:

$$\frac{O(z)}{I(z)} = \frac{b_0(z+1)^2}{a_2 z^2 + a_1 z + a_0} \qquad \text{(D-8)}$$

where

$$b_0 = (\omega_n \Delta t)^2$$ (D-9)

$$a_0 = 4 + (\omega_n \Delta t)^2 - 4\xi \omega_n \Delta t$$

$$a_1 = -8 + 2(\omega_n \Delta t)^2$$

$$a_2 = 4 + (\omega_n \Delta t)^2 + 4\xi \omega_n \Delta t$$

Applying the rules of the inverse z-transform, the associated time-domain difference equation is as follows:

$$o_k = \frac{b_0[i_k + 2i_{k-1} + i_{k-2}] - a_1 o_{k-1} - a_0 o_{k-2}}{a_2}$$ (D-10)

Similarly, if z is substituted into equation (D-6), and the results are collected, then the resulting z-transform function for the differentiating filter is as follows:

$$\frac{O(z)}{I(z)} = \frac{c_0(z^2 - 1)}{a_2 z^2 + a_1 z + a_0}$$ (D-11)

where

$$c_0 = 2\Delta t \omega_n^2$$ (D-12)

Applying the rules of the inverse z-transform, the associated time-domain difference equation is

$$\left(\frac{do}{dt}\right)_k = \frac{c_0[i_k - i_{k-2}] - a_1\left(\frac{do}{dt}\right)_{k-1} - a_0\left(\frac{do}{dt}\right)_{k-2}}{a_2}$$ (D-13)

Equations (D-10) and (D-13) are time-recursive equations with k being the discrete-time index. Because the equations are second-order, results from the two previous recursions are required at each frame. For initial startup, this condition will cause brief transients which damp out in a period of time on the order of several τ.

SECOND-ORDER ACCURATE, BACKWARDS-DIFFERENCE DIFFERENTIATOR

If no filtering of the velocity or accelerations is desired, the IIR differentiator described in the Differentiator Transfer Function and Filter Discretization sections will not work. In this case, a second-order accurate, backwards-difference differentiator with the following form is used:[7]

$$\left(\frac{do}{dt}\right)_k = \frac{3i_k - 4i_{k-1} + i_{k-2}}{2\Delta t}$$ (D-14)

VELOCITY AND ACCELERATION COMPONENTS

The range, azimuth, and elevation angles may be filtered in the program. The geocentric position components of the vehicle, xc, yc, and zc, are differentiated and filtered once for velocity components and once again for acceleration components. The velocity and acceleration components are then rotated into the local north, east, and down system of the vehicle by

$$\begin{bmatrix} V_n \\ V_e \\ V_d \end{bmatrix} = \Gamma \begin{bmatrix} V_x \\ V_y \\ V_z \end{bmatrix} \tag{D-15}$$

$$\begin{bmatrix} Acc_n \\ Acc_e \\ Acc_d \end{bmatrix} = \Gamma \begin{bmatrix} Acc_x \\ Acc_y \\ Acc_z \end{bmatrix} \tag{D-16}$$

where

$$\Gamma = \begin{bmatrix} -\sin(\lambda)\cos(\theta) & -\sin(\lambda)\sin(\theta) & \cos(\lambda) \\ -\sin(\theta) & \cos(\theta) & 0 \\ -\cos(\lambda)\cos(\theta) & -\cos(\lambda)\sin(\theta) & -\sin(\lambda) \end{bmatrix} \tag{D-17}$$

and where λ and θ is the geodetic latitude and longitude of the vehicle, respectively. If the user desires, acceleration of gravity at the vehicle altitude, g, may be subtracted from downward acceleration. The value of g can be calculated from[16]

$$g = g_o \frac{R_o^2}{(R_o + zgeoid)^2} \tag{D-18}$$

where g_o is standard acceleration of gravity, R_o is a radius of the Earth, and $zgeoid$ is the geoid altitude of the vehicle. This subtraction makes the acceleration similar to that value measured by an onboard accelerometer.

APPENDIX E

EARTH RELATIVE AND AIRDATA PARAMETER DERIVATION

The Earth-relative parameters are a function of the Earth-relative velocity components V_n, V_e, and V_d. Total Earth-relative velocity, V, is given by

$$V = \sqrt{V_n^2 + V_e^2 + V_d^2} \tag{E-1}$$

Flightpath heading, Ψ, is the horizontal angular direction the vehicle is going relative to true north. This heading has nothing to do with where the vehicle is pointed and is computed as follows:

$$\Psi = \tan^{-1}\left(\frac{V_e}{V_n}\right) \tag{E-2}$$

Flightpath angle, γ, or the vertical angular direction that the vehicle is going relative to the local horizontal is defined positive upward as

$$\gamma = \tan^{-1}\left(\frac{-V_d}{\sqrt{V_n^2 + V_e^2}}\right) \tag{E-3}$$

Airdata parameters are determined from Earth-relative parameters that are adjusted for atmospheric properties. These atmospheric properties have been entered into a table input to the "radar" program and are discussed in appendix F. For interpolation and computation purposes, the magnitude and direction of the wind and lateral pressure altitude gradient are converted into Cartesian coordinates by

$$W_n = W\cos(\Psi_w)$$
$$W_e = W\sin(\Psi_w)$$
$$\Delta H_{p\ lat_n} = \Delta H_{p\ lat}\cos(\Psi_{p\ lat}) \tag{E-4}$$
$$\Delta H_{p\ lat_e} = \Delta H_{p\ lat}\sin(\Psi_{p\ lat})$$

The true airspeed, V_∞, of the vehicle is the square root of the squares of Earth relative speed plus the windspeed expressed in feet per second for each component. Vertical winds are assumed to be zero.

$$V_\infty = \sqrt{(V_n + W_n)^2 + (V_e + W_e)^2 + V_d^2} \tag{E-5}$$

42

True Mach number, M_∞, is the true airspeed divided by the speed of sound. That is,

$$M_\infty = \frac{V_\infty}{\sqrt{k\dfrac{1000R}{M_o}(T_\infty + 273.15^\circ)}}\frac{1200\ m}{3937\ ft} \tag{E-6}$$

where T_∞ is the ambient temperature at the altitude of the vehicle; k is the ratio of specific heats for air; R is the universal gas constant; and M_o is the molecular weight of dry air. Pressure altitude from the atmospheric table is adjusted for a lateral pressure gradient by

$$H_p = H_{p\ table} + \frac{xr\Delta H_{p\ lat_n} + yr\Delta H_{p\ lat_e}}{6076.1155\dfrac{ft}{n.\ mi.}} \tag{E-7}$$

where xr and yr are determined from equations (A-25) and (A-26).

Ambient pressure, Ps_∞, is determined from pressure altitude by the U. S. Standard Atmosphere.[16] For regions of the atmosphere where the temperature has a constant lapse rate, L, the ambient pressure is

$$Ps_\infty = Ps_{\infty_{base}}\left[1 + \frac{L}{(T_{\infty_{base}} + 273.15^\circ)}(H_p - H_{p_{base}})\right]^{\frac{-g_o M_o}{RL}} \tag{E-8}$$

where the subscript *base* denotes values at the lowest altitude of the region. For regions with a constant temperature, ambient pressure is

$$Ps_\infty = Ps_{\infty_{base}}e^{\left[\frac{-g_o M_o}{R(T_\infty + 273.15^\circ)}\left(H_p - H_{p_{base}}\right)\right]} \tag{E-9}$$

The values of L, $T_{\infty_{base}}$, and $Ps_{\infty_{base}}$ are given for each atmospheric region in table E-1. For altitudes greater than those in table E-1, ambient pressure is set to zero.

Lastly, dynamic pressure, $\bar{q}$, is defined as

$$\bar{q} = \frac{k}{2}Ps_\infty M_\infty^2 \tag{E-10}$$

The values for wind magnitude, wind direction, and ambient pressure at the vehicle are determined by interpolation of the atmospheric table.

Table E-1. Constants used in equations (E-8) and (E-9).[16]

H_p, km	L, K/km	$T_{\infty_{base}}$, °C	$Ps_{\infty_{base}}$, lbf/ft²
0–11	–6.5	15.0	2116.22
11–20	0.0	–56.5	472.68
20–32	1.0	–56.5	114.3450
32–47	2.8	–44.5	18.12885
47–51	0.0	–2.5	2.31630
51–71	–2.8	–2.5	1.398035
71–84.852	–2.0	–58.5	0.082631

APPENDIX F

PROGRAM USE

This appendix gives a short history of the "radar" program and operational details of its use. The primary focus of this discussion involves the program's use at NASA Dryden.

BACKGROUND

An early version of this computer program dates back to the late 1950's and was used with the X-15 program.[*] This code, version 1.0, computed Cartesian position, altitude, total velocity, rate of climb, and radial acceleration. It used only the White Sands method for refraction correction (appendix C). Altitude was computed assuming a spherical Earth. Over the years, several new features and options were added to the program. In addition, the code was converted several times as mainframe computers were replaced with newer models. The program on the IBM computer was called version 2.0. Version 3.0 was on the CYBER computer. Version 3.0 was converted for use on the ELXSI computer as version 4.0. Version 5.0 was basically the current program implemented on the ELXSI, and version 6.0 was converted to run on a SUN 600 workstation. Versions 6.1 and 6.2 removed a few problems from version 6.0 and added a few new options. Previously, several versions of the same program existed simultaneously. In addition, each user tailored the code to fit individual needs. Inefficiencies and errors were found in the program, probably because of the lack of central control of the source code. To refurbish the program, each algorithm was investigated and derived from basic principles, and inefficiencies in the code were eliminated. Now the code, version 6.2, resides on the system level of cs1, a SUN 600 workstation using System 4.1.2, and configuration changes will be tracked.

EXECUTABLE AND SOURCE CODES

For the computer cs1 at NASA Dryden, the files for the program reside in the directory, **/dryden/cs1/radar**. The executable file **radar** handles input—output definitions and executes the FORTRAN code. The executable FORTRAN code, **radar.source.6.2**, is generated from the source code, **radar.source.6.2.f**, by running **radar.bind**.

PREPARING RAW DATA FOR THE SUN 600 COMPUTER

The four possible sources for the raw radar data are as follows:

- Flight Data Access System (FDAS)[2] at NASA Dryden.

- Nine-track magnetic tape supplied by Western Aeronautical Test Range (WATR).

- Engineering units range, azimuth, elevation in an unformatted file.

- Geocentric Cartesian coordinate data in an unformatted file.

---

[*]Marcalus, Vincent J., NASA-FRC Data Reduction Requirements for High Range Radar Data, undated working paper.

Figure F-1 shows a flowchart for the radar program. The following subsections describe each source and provide specific directions for preparing the data for use on the SUN 600 computer called cs1 at NASA Dryden.

Figure F-1. Flowchart of the "radar" program, version 6.2.

Flight Data Access System Data

If the raw data resides on the FDAS, the user needs to copy the data into a working directory using the GetFdas utility.[*] The steps to retrieve data using GetFdas are outlined next.

1. Enter the utility with the command

getfdas

2. Select the flight project with the command

project <flight-project>

3. Enter the appropriate identification or password if one is required for your project.

4. Select the appropriate flight with the command

flight <flight-number>

5. Complete the parameters command with

parameters range_cts_## azimuth_cts_## elevation_cts_##

where ## is the radar site number. Some vehicles are tracked by multiple radars simultaneously, and some projects have the main vehicle tracked by one radar and the chase vehicle tracked by a different radar. The "radar" program can analyze the data set from only one radar at a time. Valid radar site numbers for Edwards AFB, California, are 34 (primary NASA Dryden radar), 05 (backup NASA Dryden radar), and 38 and 41 (Air Force Flight Test Center, radars).

6. Enter the write command with

write <prefix>.raw.radar unc3

where <prefix> is a descriptive name for the aircraft, flight, and maneuver, for example, **f104.1228.ad**. This command produces the file **<prefix>.raw.radar** in your working directory in unc3 format.[2]

7. Enter the time command with

times hh.mm.ss.msec - hh.mm.ss.msec sync=radar_##

where the first hh.mm.ss.msec is the hours, minutes, seconds, and milliseconds of the beginning of the data of interest, and the second time is the stop time. Some of the data on the FDAS are in Greenwich mean time (G.m.t.),

---

*Maine, Richard E., User's Manual for GetFdas; Version 0.72, Apr. 30, 1993, working paper.

but the majority of these data are in local times. A maximum of 75,000 time points may be used for each run. This maximum corresponds to 60 min of data at 20 samples/sec with extra padding for filtering start-up transients, lags, and spike removal. As stated in appendix D, start-up transients die out on the order of several lag constants. Spike removal and filtering any parameter causes samples to be lost at the end of the data. Such losses result from the time shifting of the lag (equation (D-4)); therefore, the requested start time of the data should be before the required start time. In turn, the stop time of the data should be after the required stop time when filtering is performed. For the default-filtering frequencies shown in table F-1, 3.150 sec of extra data are needed to account for the lags. Spike removal requires one-half of a window of extra data points, which is 2.500 sec for the default window size and input sample rate.

8. Exit the GetFdas utility and return to cs1's operating system by entering the command

<div align="center">

quit

</div>

<div align="center">

Table F-1. Namelist parameters for **<prefix>.radar.setup** file.

</div>

Namelist	Parameter	Description	Type	Default
date	**month**	Month of flight	Int*4	None
	day	Date of flight	Int*4	None
	year	Year of flight	Int*4	None
input	**prefix**	File name prefix for all input–output files	Char*66	None
	istart	Start hr, min, sec, msec time	Int*4(4)	None
	istop	Stop hr, min, sec, msec time	Int*4(4)	None
	izulu	Number of offset hours, 7 for G.m.t to P.d.t., 8 for G.m.t. to P.s.t.	Int*4	None
indat	**spikes**	.true. to remove spikes	Logic*4	.false.
	window	Number of points in spike window	Int*4	100
	sigma	Number of standard deviations for spike removal	Real*8	3.
	hlv	Hold-last-value for missing data	Logic*4	.false.
	xi	Damping ratio of filters	Real*8	$\sqrt{2}/2$
	wb1	Position-filtering break frequency, Hz	Real*8	0.5
	wb2	Velocity-filtering break frequency. Hz	Real*8	0.25
	wb3	Acceleration-filtering break frequency, Hz	Real*8	0.125
	gravity	Is g to be subtracted from acceleration down?	Logic*4	.true.
	spsin	Sample rate of input	Real*8	20.

Namelist	Parameter	Description	Type	Default
	nprint	Print-thinning factor	Int*4	40
amb	**corref**	.true. for refraction corrections	Logic*4	.true.
	emin	*el* below which gradient refraction is used	Real*8	7°
	tdry	Radar site dry bulb temperature	Real*8	59 °F
	twet	Radar site wet bulb temperature	Real*8	59 °F
	pamb	Radar site atmospheric pressure	Real*8	27.25 in. Hg.
	reft	.true. if refraction table is used	Logic*4	.false.
	nref	Number of entries in refraction table	Int*4	0
	zmin	Altitude below which gradient refrection is not truncated	Real*8	10,000. ft
	ls	Length of gradient refraction segments	Int*4	1,000 ft
	grellip	.true. if the full ellipsoid Earth model is to be used in gradient refraction corrections	Logic*4	.false.
radsite	**sitlat**	Radar site geodetic latitude	Real*8	34.96081°
	sitlng	Radar site longitude	Real*8	−117.91150°
	sith	Radar site ellipsoid altitude	Real*8	2563.200 ft
	sitgs	Radar site geodetic separation	Real*8	−99.393 ft
	zbias	Altitude bias, *zgeoid* = *h* − **sitgs** − **zbias**	Real*8	0
	a	Semimajor axis of Earth	Real*8	20925604.47 ft
	b	Semiminor axis of Earth	Real*8	20855444.88 ft
	mlas	Maximum mislevel, arc sec	Real*8	0
	mlsir	Azimuth of maximum up mislevel, deg	Real*8	0°
opt	**atm**	.true. if atmospheric table used	Logic*4	.false.
	numbp	Number of entries in atmospheric table	Int*4	0
	binout	.true. if Real*8 binary output desired	Logic*4	.false.
	binraw	.true. if Real*8 binary raw *t, r, az, el* data are to be read in	Logic*4	.false.
	taperaw	.true. if data on WATR 9-track tape	Logic*4	.false.
	unc3raw	.true. if data on FDAS, unc3 format	Logic*4	.true.
	xyz	.true. if Real*8 binary raw *t, xc, yc, zc* data are to be read in	Logic*4	.false.
	thin	Thinning factor for output	Int*4	1

Western Aeronautical Test Range Nine-Track Tape Data

If the radar data are from Edwards AFB, California, but are not on the FDAS, then the raw radar data are probably on 9-track magnetic tape in encoded binary format supplied by the WATR. Most of these tapes were written at a density of 800 bpi, and the rest were written at a density of 6250 bpi. The tape drive on the computer named cs2 will automatically select the proper tape density. These data need to be copied from magnetic tape to the working directory. Steps for copying these data are as follows:

1. Call the computer operator.

2. Ask to have the tape mounted on the cs2 tape drive.

3. Give the operator the tape number, for example, **3679f**.

4. Be sure to specify "no ring" to make the tape write protected.

5. Read the tape using the command

rsh -l tapeuser -n cs2 dd if=/dev/rst3 ibs=900 > <prefix>.raw.radar

from the working directory.

6. Verify that this procedure produced the file **<prefix>.raw.radar** in the working directory.

7. Call the operator back to have the tape removed from the tape drive.

Raw Range, Azimuth, Elevation Data

If the data come from a radar that is not located at Edwards AFB, California, provide a binary file with time (seconds after midnight), range (feet), azimuth (degrees clockwise from true north), and elevation (degrees above local horizon) on each record and without a header. These four parameters must be in 8-byte unformatted words, as is generated by an unformatted write command in FORTRAN with double precision variables. Name this file **<prefix>.raw.radar** located in the working directory.

Raw Cartesian Coordinate Data

If the raw data are Cartesian coordinate position data referenced to the center of the Earth, provide an 8-byte unformatted word file with time (seconds after midnight), xc, yc, and zc (feet) on each record with no header. This coordinate system is described in appendix A. Name this file **<prefix>.raw.radar** located in the working directory.

As shown in figure F-1, one of the four input sources named **<prefix>.raw.radar** is required. The file **<filename>.radar.setup** controls which of the four sources is used for a particular run.

CHOOSING RADAR PROGRAM OPTIONS

Generate the **<prefix>.radar.setup** file which contains all the option settings to execute the radar program using namelist and tables. An example file is given at the bottom of this subsection. Ensure that the first column is blank.

50

The first record of this file is an 80-character line of text that will be the header for printed output. The namelists start on the second record. Table F-1 lists these namelists, parameters, descriptions, and default values. Note that namelists "date" and "inpt" have no defaults and must always be included in the file. The parameter **prefix** should be set to <prefix>. This setting allows the program to find the appropriate input files. The refraction table, if one is desired (that is, if **reft** = .true.), follows the namelists. If airdata parameters are desired (that is, if **atm** = .true.) the atmospheric table is last in the file (fig. F-1). The namelist parameters and the table formats are discussed next.

"date", "inpt", and "indat"—The parameters of these namelists are adequately listed in table F-1, but a few caveats exist for the times and filtering break frequencies. There is a maximum of 75,000 time points/run, which corresponds to 60 min of data at 20 samples/sec with extra padding for filtering. If an interval is requested that exceeds the 75,000 time points, an error message will be printed and the program will stop. The start time should take into account start-up transients of the filters. The stop time is the actual desired stop time. The program will automatically read in enough data after the stop time to account for the filtering lags.

"izulu"—If the raw data are from the WATR 9-track tape, time is in G.m.t., and **izulu** needs to be set to the hour offset between G.m.t. and the desired time zone. Data on the FDAS are generally in local time, so **izulu** would be zero.

hlv—If gaps exist in the input data, the program will fill in the missing data. Data are generated by using hold-last-rate on the previous data as the default. The missing data can be generated by hold-last-value by setting **hlv** true, but remember that the velocities and accelerations will be adversely affected.

wb1—If the position filtering break frequency, **wb1**, is set to zero, no filtering is performed.

wb2 or wb3—If the break frequencies for either velocity or acceleration, **wb2** or **wb3**, are set to zero, a second-order accurate, backwards-difference differentiator is used with no filtering for that derivative.

corref—The parameter **corref** determines if atmospheric refraction corrections (both gradient refraction and White Sands methods) are performed.

emin—Parameter **emin** is the measured elevation angle below which the gradient refraction method is used.

If **emin** = −90°, use White Sands method.

If **emin** = 90°, use the gradient refraction method.

Giving an intermediate value to **emin** causes the White Sands method to be used for high-elevation angles where it is quite accurate, and the gradient refraction method to be used for low-elevation angles. Using the New Edwards curve, figure 4 can be used for Edwards AFB, California, to decide what value of **emin** is appropriate for a particular application. Note that errors will be larger than those in figure 4 when the range exceeds 600,000 ft. If refraction corrections are to be performed, either the radar site atmospheric properties or a refraction table must be provided. If both are in the <prefix>.radar.setup file, the refraction table is used.

tdry, twet, and pamb—The radar site atmospheric parameters are **tdry, twet,** and **pamb.** If the values of these three parameters are physically impossible, a warning will be printed, and the program will stop.

reft and nref—Parameters **reft** and **nref** are set if a refraction table is included for input. This table will have a column of geometric geoid altitude (above mean sea level) and a second column of refractivity (sometimes called "N" units). Table F-2 gives an example of a refractivity table. This table must be in increasing order of altitude and follow the namelists (fig. F-1). Because the program extrapolates refractivity when the desired value is outside the bounds of the table, the first two and last two entries in the table must exhibit the same trend as the rest of the data.

Table F-2. Example of refractivity table (Pt. Arguello, California, July 17, 1991, 1630 G.m.t.).

zgeoid, ft	N	*zgeoid*, ft	N
1,000	323	33,000	94
2,000	311	34,000	91
3,000	293	35,000	87
4,000	274	36,000	83
5,000	241	37,000	80
6,000	233	38,000	76
7,000	229	39,000	72
8,000	226	40,000	68
9,000	222	41,000	65
10,000	217	42,000	63
11,000	209	43,000	60
12,000	200	44,000	57
13,000	191	45,000	54
14,000	181	46,000	52
15,000	174	47,000	50
16,000	168	48,000	48
17,000	162	49,000	46
18,000	156	50,000	44
19,000	151	51,000	42
20,000	145	52,000	40
21,000	141	53,000	38
22,000	136	54,000	36
23,000	131	55,000	34
24,000	127	56,000	33
25,000	123	57,000	31
26,000	119	58,000	30
27,000	115	59,000	28
28,000	111	60,000	27
29,000	108	61,000	25
30,000	104	62,000	24
31,000	101	63,000	23
32,000	97	98,500	4

This information is usually given in 1000-ft increments. The White Sands method only uses the refractivity at the altitude of the radar site.

zmin, ls, and grellip—The parameters **zmin**, **ls**, and **grellip** are used to control the gradient refraction method.
- The **zmin** is the geoid altitude below which the truncation algorithm is not used. This truncation algorithm assumes an exponential decay of refractivity with altitude. Near the ground and especially in inversion layers, the refractivity may be irregular (fig. 2). Appendix C discusses this subject in additional detail.

- The **ls** is the approximate length of the segment used in the gradient refraction method. The accuracy of the gradient refraction method depends on **ls**, and its optimum value depends on the roundoff and truncation errors of the computer. For the SUN 600 computer at NASA Dryden, a value of ls = 1000 ft is generally used although this value may not be the optimum. This value was selected because data from balloon profiles of refractivity come at 1000-ft intervals.

- The **grellip** controls the Earth model used during the gradient refraction method. If **grellip** = .false., the Earth model is spherical. If **grellip** = .true., the Earth model is the ellipsoid. To date, no significant differences in refraction corrections using the two settings of **grellip** have been observed, but possibly it could be significant at extreme ranges. Using the ellipsoid model during the gradient refraction method increases computation time tremendously.

sitlat, sitlng, sith, and sitgs—These parameters represent the geodetic latitude, longitude, ellipsoid altitude, and geodetic separation, respectively, of the radar site for the Earth model described by the parameters a and b. The defaults are for radar 34 at Edwards AFB, California, in the WGS 84 system. Table F-3 gives radar site positions for several installations in the WGS 84 system. Table 1 gives values for a and b in several systems. Entering values for **sitlat, sitlng, sith, sitgs, a,** or **b** has no effect for the FDAS or WATR input formats. When the raw data are from the FDAS or the WATR 9-track tape, the radar site coordinates in the WGS 84 system are automatically entered to the program for any of the four radars at Edwards AFB, California.

Table F-3. California radar site coordinates in WGS84 system.

Radar site	Latitude, deg	Longitude, deg	h_s, ft	g_s, ft	$zgeoid_s$, ft
Edwards 34	34.96081	−117.91150	2563.200	−99.393	2662.593
Edwards 05	34.95774	−117.91187	2538.699	−99.403	2638.102
Edwards 38	34.96961	−117.92941	2605.359	−99.304	2704.663
Edwards 41	34.97045	−117.93056	2623.771	−99.298	2723.069
Pt. Mugu 003004	34.12289	−119.15475	−77.211	−121.027	43.816
Pt. Pillar 213002	37.49784	−122.49970	61.030	−108.917	169.947
Pt. Pillar 213003	37.49687	−122.49667	7.192	−108.881	116.073
San Nicholas Is. 013003	33.24769	−119.52074	809.700	−122.040	931.740
Vandenberg 023001	34.58276	−120.56157	2059.281	−113.510	2172.791
Vandenberg 023002	34.58305	−120.56111	2059.310	−113.500	2172.811
Vandenberg 023003	34.66586	−120.58144	288.871	−113.412	402.283
Vandenberg 033001	34.75825	−120.62712	85.298	−113.103	264.019
Vandenberg 033701	34.77492	−120.53607	404.530	−112.674	517.204

zbias—The user can bias the altitude using the **zbias** parameter. This function may be desirable if the geoid separation at the radar site differs significantly from the geoid separation at the location of the vehicle. To output altitude as ellipsoid altitude, make **zbias = –sitgs**.

mlas and mldir—These parameters allow corrections for radar pedestal mislevel. It is assumed that the pedestal is tilted by the number of arc seconds in **mlas** and that the azimuth of the high side of the pedestal is given by **mldir**.

atm—This parameter is set to .true. if an atmospheric table is input so that airdata parameters can be calculated. This table consists of seven columns, an example of which is given in table F-4, and is placed at the end of the file (fig. F-1). The first column is geometric altitude (above mean sea level) in feet, $zgeoid$, and the second is the corresponding pressure altitude in feet, $H_{p\ table}$, for a weather analysis above the radar site. Ambient temperature, T_∞, is shown the third column. The fourth and fifth columns include windspeed in knots, W, and wind direction, Ψ_w. The wind direction is in degrees from true north and describes the direction from which the wind blows, so a north wind blows from north to south, and $\Psi_w = 0°$. The sixth and seventh columns list lateral pressure altitude gradient and direction, $\Delta H_{p\ lat}$ and $\Psi_{p\ lat}$. The lateral pressure altitude gradient is the number of feet that pressure altitude changes per nautical mile, and direction is the direction of decrease of pressure. As a result, if a low pressure area is due north of the radar site, then $\Psi_{p\ lat} = 0°$. This table must be arranged in increasing order of geometric altitude. If values outside the range of the table are sought, the nearest values of the table are used.

numbp—This parameter represents the number of entries (rows) in the atmospheric table.

Table F-4. Sample atmospheric table for radar 34, at Edwards, California, on June 13, 1988.

$zgeoid$, ft	$H_{p\ table}$, ft	T_∞, °C	W, kn	Ψ_w, deg	$\Delta H_{p\ lat}$, deg ft/n. mi.	$\Psi_{p\ lat}$, deg
2,302	2,275	30.0	03	085	0.10	250
3,330	3,243	25.5	04	074	0.10	170
4,133	4,003	22.7	10	074	0.10	165
4,956	4,781	21.5	13	080	0.20	160
6,145	5,902	20.0	12	072	0.20	160
10,354	9,882	8.8	09	145	0.25	235
13,597	12,977	–0.6	06	275	0.25	360
15,806	15,079	–0.2	11	310	0.30	040
19,201	18,289	–8.1	14	313	0.40	057
24,759	23,574	–21.4	20	306	0.50	032
28,800	27,469	–31.5	43	300	0.55	032
31,495	30,065	–38.3	34	300	0.55	032
33,045	31,570	–42.0	33	301	0.65	030
35,533	33,999	–48.8	38	300	0.67	027
38,258	36,679	–55.0	39	300	0.70	020
39,232	37,647	–56.5	44	294	0.74	020
40,244	38,662	–58.8	50	300	0.76	020
41,855	40,284	–59.4	45	301	0.74	020

The program uses the distance north and east of the radar site, *xr* and *yr*, from equations (A-25) and (A-26). Because these quantities originate at the radar site, the atmospheric table should be referenced to the specific radar site geographically. If the atmospheric table is not referenced to the radar site, the radar data must first be processed without atmospheric input to give geocentric position. Then using the geocentric position as input, run the program again with the radar site respecified as the origin of the atmospheric data.

binraw, taperaw, unc3raw, xyz, and binout—These parameters are explained in table F-1 and control which input source is used and whether binary output is generated. Note that although binary output takes up a great deal more memory than the normal compressed output (which is in cmp3 format)[2], it retains its full 8-byte word. The cmp3 format output retains only the three most significant bytes. This level of precision is acceptable for most parameters. On the other hand for such parameters as Cartesian position from the center of the Earth, latitude, and longitude, a significant amount of resolution is lost when the compressed format is used.

thin—This last parameter in the namelist is the requested thinning factor for the output. This parameter has no effect on the filters or differentiation and is only used for the output routines.

Figure F-2 shows an example radar.setup file. This file will process data for flight 1228 of the F104 aircraft (Lockheed Corporation, Burbank, California) which occurred on June 13, 1988. Four and one-half minutes of data are analyzed from 11:33:32 to 11:38:02 local time, and a 7-hr offset exists between P.d.t. and G.m.t. The filtering frequencies have been changed from the defaults, and the radar site weather conditions are entered for atmospheric refraction corrections. Radar site information will be entered automatically when the raw data are read, but manual entry of the namelist name is still required in this setup file. An atmospheric table has been provided with 18 breakpoints, so airdata quantities will be computed. The input is from the WATR 9-track tape, and a binary output file will be generated. Entering the command

man radar

on cs1 gives an abbreviated set of these instructions and this example.

RUNNING THE RADAR PROGRAM

Now that the input files have been created, begin the radar program by typing

radar <prefix>.radar.setup

in the working directory. If the program will take a while to run (for example, if the gradient refraction is used), then consider using this program in another window or in the background. After successful use of the program, the compressed output in cmp3 format[2] will be in **<prefix>.radar.out**. The binary output, if requested, will be in **<prefix>.radar.out.bin** (fig. F-1). If an atmospheric reference table is used, all parameters given in table F-5 are output. If an atmospheric reference table is not provided, only channels 0 through 29 are output. Most of the output parameter names have an "r" prefix to help distinguish these radar-derived results from results derived from aircraft-calibrated parameters, global-positioning systems, or inertial navigation systems. The data can be examined using a plotting program. A text output will be created called **<prefix>.radar.print.** An abbreviated version of the text output is sent to standard output, which is the monitor when the program is run interactively. Multiple data sets may be analyzed simultaneously from the same directory if each has a unique **prefix.**

55

```
radar data for F104 flt1228 a/c, radar #34
$date month=06, day=13, year=1988 $
$inpt prefix='f104.1228', istart=11,33,32,000, istop=11,38,02,000, izulu=7 $
$indat wb1=0.2, wb2=0.1, wb3=0.05 $
$amb tdry=86.0, twet=59.0, pamb=27.17 $
$radsite $
$opt atm=.true., numbp=18, binout=.true., taperaw=.true. $
        2302.,  2275.,  30.0, 03., 085.,0.10, 250.
        3330.,  3243.,  25.5, 04., 074.,0.10, 170.
        4133.,  4003.,  22.7, 10., 074.,0.10, 165.
        4956.,  4781.,  21.5, 13., 080.,0.20, 160.
        6145.,  5902.,  20.0, 12., 072.,0.20, 160.
       10354.,  9882.,   8.8, 09., 145.,0.25, 235.
       13597., 12977.,  -0.6, 06., 275.,0.25, 360.
       15806., 15079.,  -0.2, 11., 310.,0.30, 040.
       19201., 18289.,  -8.1, 14., 313.,0.40, 057.
       24759., 23574., -21.4, 20., 306.,0.50, 032.
       28800., 27469., -31.5, 43., 300.,0.55, 032.
       31495., 30065., -38.3, 34., 300.,0.55, 032.
       33045., 31570., -42.0, 33., 301.,0.65, 030.
       35533., 33999., -48.8, 38., 300.,0.67, 027.
       38258., 36679., -55.0, 39., 300.,0.70, 020.
       39232., 37647., -56.5, 44., 294.,0.74, 020.
       40244., 38662., -58.8, 50., 300.,0.76, 020.
       41855., 40284., -59.4, 45., 301.,0.74, 020.
```

Figure F-2. Sample **<prefix>.radar.setup** file for flight 1228 of the F104 aircraft, June 13, 1988. (The first column of this file is blank.)

MEMORY

On the SUN 600 computer, the FORTRAN source code takes up 89 kilobytes of memory, and the compiled code takes up 385 kilobytes of memory. For 30 min of data at 20 samples/sec, the approximate maximum file sizes are as follows:

- 84 kilobytes for the standard output saved to a file

- 656 kilobytes for **<prefix>.radar.print**

- 3.2 megabytes for **<prefix>.radar.out**

- 11 megabytes for **<prefix>.radar.out.bin**

- 23 megabytes for the assorted scratch files.

Each scratch file is automatically deleted when the program finishes using that file. File sizes are smaller when shorter time segments are used and if the airdata parameters are not desired. The **<prefix>.raw.radar** file may require several megabytes. Table F-5 shows the output parameters.

Table F-5. Output parameters.

No.	Parameter	Description	Equation
0.	time	Local time after midnight, sec	—
1.	rraw	Range, counts	—
2.	araw	Azimuth, counts	—
3.	eraw	Elevation, counts	—
4.	reng	Range, no corrections, ft	—
5.	aeng	Azimuth, no corrections, deg	—
6.	eeng	Elevation, no corrections, deg	—
7.	rfilt	Range, spikes removed and filtered, ft	—
8.	afilt	Azimuth, spikes removed and filtered, deg	—
9.	efilt	Elevation, spikes removed and filtered, deg	—
10.	rcor	Range, rfilt corrected for refraction, ft	—
11.	ecor	Elevation, efilt corrected for refraction, deg	—
12.	rxc	Distance from center of Earth along equitorial plane toward 0° longitude, ft	(A-20)
13.	ryc	Distance from center of Earth along equitorial plane toward 90° east longitude, ft	(A-20)
14.	rzc	Distance from center of Earth toward north pole, ft	(A-20)
15.	rxr	Distance north of radar site on ellipsoid Earth, ft	(A-24)
16.	ryr	Distance east of radar site on ellipsoid Earth, ft	(A-25)
17.	rz	Geometric altitude above mean sea level (geoid), $zgeoid = h -$ **sitgs** $-$ **zbias**, ft	(B-40) with bias
18.	rglat	Geodetic latitude, deg	(A-22)
19.	rgclat	Geocentric latitude, deg	(A-21)
20.	rglong	Longitude, deg	(A-23)
21.	rvn	Velocity north filtered, ft/sec	(D-15)
22.	rve	Velocity east filtered, ft/sec	(D-15)
23.	rvd	Velocity down filtered, ft/sec	(D-15)
24.	ran	Acceleration north filtered, ft/sec^2	(D-16)
25.	rae	Acceleration east filtered, ft/sec^2	(D-16)
26.	rad	Acceleration down filtered, local gravity may be subtracted, ft/sec^2	(D-16 and D-18)
27.	rvtot	Earth relative total velocity, ft/sec	(E-1)
28.	rfph	Flightpath heading, deg	(E-2)
29.	rfpa	Flightpath angle, deg	(E-3)
		Atmospheric-derived parameters	
30.	rwindmag	Wind magnitude, ft/sec	—
31.	rwinddir	Wind direction from true north, deg	—
32.	rpsinf	Ambient pressure, lbf/ft	(E-8 and E-9)
33.	rtinf	Ambient temperature, °R	—
34.	rvinf	True airspeed, ft/sec	(E-5)
35.	rminf	Mach number	(E-6)
36.	rqbar	Dynamic pressure, lbf/ft	(E-10)
37.	rhp	Pressure altitude, corrected for lateral pressure gradient, ft	(E-7)

APPENDIX G

NOMENCLATURE

A	scale height constant for equation (C-7), m
AFB	Air Force Base
AFFTC	Air Force Flight Test Center, Edwards, California
AN/FPS-16	Army-Navy/Fixed Position System radar
Acc	vehicle acceleration, ft/sec^2
a	ellipsoid semimajor axis, ft
a, b, c, d; f, g	refractivity constants for equations (C-3) and (C-4)
az	azimuth angle, deg
a_0, a_1, a_2, b_0, c_0	filter constants
a2, b2, c2	coefficients of second-order form of quartic equation
B	scale height constant for equation (C-7), m
b	ellipsoid semiminor axis, ft
b_c, c_c, d_c	coefficients of resolvent cubic equation
bpi	bits per inch
b_q, c_q, d_q, e_q	coefficients of quartic equation
C	dummy variable
C	scale height constant for equation (C-7), m
Char	character FORTRAN variable
c_o	speed of light in a vacuum, ft/sec
D	downrange distance from radar site, ft or yd
d	distance from ellipsoid, ft
$delt$	time interval for gradient refraction segment, sec
e	eccentricity
el	elevation angle, deg
es	saturation vapor pressure, in. Hg.
ev	vapor pressure, in. Hg.
FDAS	Flight Data Access System
G.m.t.	Greenwich mean time
GPS	Global Positioning System
g	acceleration of gravity at the vehicle, ft/sec^2

g_o	standard acceleration of gravity, 32.1740 ft/sec^2 or 9.80665 m/sec^2
gs	geoid separation, ft
H	scale height, m
Hp	pressure altitude, ft
$H_{p\ table}$	pressure altitude from atmospheric table, ft
h	geometric ellipsoid altitude, ft
I	transformed input function
IIR	infinite impulse response
INS	inertial navigation system
Int	integer FORTRAN variable
i	time domain input function
ia	internal Earth angle, deg
J	equation (B-2)
j	imaginary number, $\sqrt{-1}$
$K_{1_\ell}, K_{2_\ell}, K_{1_r}, K_{2_r}$	White Sands method coefficients
k	ratio of specific heats for air, 1.4
L	Laplace transform
L	temperature lapse rate, K/km
LSB	least significant bit
Logic	logical FORTRAN variable
Ls	lower segment length, ft
ls	gradient refraction segment length when $\eta = 1$, ft
M	magnitude
M_o	molecular weight of dry air, 28.9644 gm/mole
Ms	middle segment length, ft
M_∞	true free-stream Mach number
$\overline{M}_n$	average remaining segment length, ft
m, n	coefficients of linear solution to quartic equation
m.s.l.	mean sea level
N	refractivity
NASA	National Aeronautics and Space Administration
n	segment number
ns	number of segments

O	transformed output function
o	time domain output function
P.d.t.	Pacific daylight time
P.s.t.	Pacific standard time
Ps_∞	ambient pressure, lbf/ft²
ps	radar site atmospheric pressure, in. Hg.
p, q	coefficients of reduced cubic equation
$\bar{q}$	dynamic pressure, lbf/ft²
R	universal gas constant, 8.31432 kg-m² /(K-mole-sec²)
Real	real FORTRAN variable
Re	local radius of curvature of the Earth at the radar site, ft
R_o	radius of the Earth for g calculation, 20,855,531.5 ft
r	ratio of reduced cubic and trigonometric reduced cubic equation solutions
r	range, ft
rh	relative humidity, percent
S	dummy variable
s	radar site vertical vector
s	Laplace transform variable
T_s	dry bulb temperature, °R or °F
T_∞	ambient temperature, °C or °R
$Twet_s$	wet bulb temperature, °R or °F
t	time, sec
t_c	variable of trigonometric reduced cubic equation
Us	upper segment length, ft
u	ellipse major coordinate, ft
V	Earth relative velocity, ft/s
V_∞	true airspeed, ft/sec
v	local vertical vector
v	ellipse minor coordinate, ft
W	windspeed, ft/sec or kn
WATR	Western Aeronautical Test Range
WGS	World Geodetic Survey
w	width of radar segment (separation between beams), ft

60

x, y, z	point on ellipsoid, ft
xc, yc, zc	Cartesian distance from the center of the Earth, ft
x_l, y_l, z_l	radar site local north, east, and down coordinates, ft
x_q	variable of quartic equation
xr	distance from the radar site north to the latitude of the piercing point, ft
y_c	variable of resolvent cubic equation
yr	distance from the radar site east to the longitude of the piercing point, ft
Z	vertical distance from radar site, ft or yd
z	discrete-time Fourier transform variable
z_c	variable of reduced cubic equation
ze	geoid altitude estimate, ft
$zgeoid$	geometric altitude above mean sea level (geoid), ft

Subscripts

base	value at the lowest altitude of the region
d	down component
e	east component
k	sample number
m	measured
min	minimum
n	north component
r	corrected for atmospheric refraction
s	radar site
x, y, z	geocentric coordinates
$x_\oplus, y_\oplus, z_\oplus$	piercing point coordinates from center of Earth, ft

Superscripts

'	values scaled by 1/a
"	approximated

Symbols

α	Lagrange multiplier
β	reduced latitude, deg
Γ	rotational matrix
γ	flightpath angle, deg
Δ	discriminant of reduced cubic equation

61

$\Delta H_{p\ lat}$	lateral pressure altitude gradient magnitude, ft/n. mi
Δel	elevation angle error, army mils
Δh_n	estimate of altitude of the target above the current segment, ft
Δr	range error, yd
Δt	sample interval, sec
δ	turning angle, deg
$\delta_{n_{rem}}$	total remaining turning, deg
$\bar{\delta}_{n_{rem}}$	average remaining turning angle, deg
η	index of refraction
θ	longitude, deg
λ	geodetic latitude, deg
λ_c	geocentric latitude, deg
ξ	damping ratio
σ	standard deviation
τ	lag, sec
ϕ	phase angle, deg
Ψ	flightpath heading from true north, deg
$\Psi_{p\ lat}$	direction of lateral pressure gradient (towards pressure decrease), deg
Ψ_w	wind direction from true north (from which wind blows), deg
ω	frequency, Hz
ω_n	natural frequency, Hz
$\oplus$	ellipsoid piercing point
$\angle$	trigonometric solution angle, deg

Namelists

date

day	day of flight
month	month of flight
year	year of flight

inpt

istart	data start time
istop	data stop time
izulu	number of offset hours
prefix	prefix of the names of the radar files

indat

gravity	logical for local gravity calculation
hlv	logical for hold-last-value for missing data
nprint	printing thinning factor
sigma	number of standard deviations for spike removal
spikes	logical for spike removal
spsin	sample rate of input
wb1	position-filtering break frequency, Hz
wb2	velocity-filtering break frequency, Hz
wb3	acceleration-filtering break frequency, Hz
window	number of points in spike removal window
xi	filter-damping ratio

amb

corref	logical for refraction corrections
emin	namelist parameter regulating refraction corrections, deg
grellip	logical for Earth model used in refraction correction
ls	segment length for gradient refraction method, ft
nref	number of rows in refraction table
pamb	ambient pressure at radar site, in. Hg.
reft	logical for refraction table
tdry	dry bulb temperature at radar site, °F
twet	wet bulb temperature at radar site, °F
zmin	namelist parameter regulating truncation algorithm, ft

radsite

a	ellipsoid semimajor axis, ft
b	ellipsoid semiminor axis, ft
mlas	maximum mislevel, arc sec
mldir	azimuth of maximum up mislevel, deg
sitgs	geoid separation at radar site, ft
sith	ellipsoid altitude of radar site, ft
sitlat	geodetic latitude of radar site, deg
sitlng	longitude of radar site, deg
zbias	altitude bias, ft

opt

atm	logical for atmospheric table
binout	logical for 8-byte word binary output data
binraw	logical for 8-byte word binary raw input data
numbp	number of rows in atmospheric table
taperaw	logical for WATR 9-track tape raw input data
thin	output-thinning factor
unc3raw	logical for Flight Data Access System input data, unc3 format
xyz	logical for Cartesian input data

REPORT DOCUMENTATION PAGE

Public reporting burden for this collection of information is estimated to average 1 hour per response, including the time for reviewing instructions, searching existing data sources, gathering and maintaining the data needed, and completing and reviewing the collection of information. Send comments regarding this burden estimate or any other aspect of this collection of information, including suggestions for reducing this burden, to Washington Headquarters Services, Directorate for Information Operations and Reports, 1215 Jefferson Davis Highway, Suite 1204, Arlington, VA 22202-4302, and to the Office of Management and Budget, Paperwork Reduction Project (0704-0188), Washington, DC 20503.

1. AGENCY USE ONLY (Leave blank)	2. REPORT DATE August 1995	3. REPORT TYPE AND DATES COVERED Technical Paper

4. TITLE AND SUBTITLE

FORTRAN Program for Analyzing Ground-Based Radar Data: Usage and Derivations, Version 6.2

6. AUTHOR(S)

Edward A. Haering, Jr., and Stephen A. Whitmore

5. FUNDING NUMBERS

WU 505-68-50

7. PERFORMING ORGANIZATION NAME(S) AND ADDRESS(ES)

NASA Dryden Flight Research Center
P.O. Box 273
Edwards, California 93523-0273

8. PERFORMING ORGANIZATION REPORT NUMBER

H-1892

9. SPONSORING/MONOTORING AGENCY NAME(S) AND ADDRESS(ES)

National Aeronautics and Space Administration
Washington, DC 20546-0001

10. SPONSORING/MONITORING AGENCY REPORT NUMBER

NASA TP-3430

11. SUPPLEMENTARY NOTES

12a. DISTRIBUTION/AVAILABILITY STATEMENT

Unclassified—Unlimited
Subject Category 61

12b. DISTRIBUTION CODE

13. ABSTRACT (Maximum 200 words)

A postflight FORTRAN program called "radar" reads and analyzes ground-based radar data. The output includes position, velocity, and acceleration parameters. Airdata parameters are also provided if atmospheric characteristics are input. This program can read data from any radar in three formats. Geocentric Cartesian position can also be used as input, which may be from an inertial navigation or Global Positioning System. Options include spike removal, data filtering, and atmospheric refraction corrections. Atmospheric refraction can be corrected using the quick White Sands method or the gradient refraction method, which allows accurate analysis of very low elevation angle and long-range data. Refraction properties are extrapolated from surface conditions, or a measured profile may be input. Velocity is determined by differentiating position. Accelerations are determined by differentiating velocity. This paper describes the algorithms used, gives the operational details, and discusses the limitations and errors of the program. Appendixes A through E contain the derivations for these algorithms. These derivations include an improvement in speed to the exact solution for geodetic altitude, an improved algorithm over earlier versions for determining scale height, a truncation algorithm for speeding up the gradient refraction method, and a refinement of the coefficients used in the White Sands method for Edwards AFB, California. Appendix G contains the nomenclature.

14. SUBJECT TERMS

Airdata, Atmospheric refraction, Computer program, Derivations, FORTRAN, Geodetics, Radar

15. NUMBER OF PAGES
65

16. PRICE CODE
AO4

17. SECURITY CLASSIFICATION OF REPORT	18. SECURITY CLASSIFICATION OF THIS PAGE	19. SECURITY CLASSIFICATION OF ABSTRACT	20. LIMITATION OF ABSTRACT
Unclassified	Unclassified	Unclassified	Unlimited

REFERENCES

[1]Ehernberger, L.J., Edward A. Haering, Jr., Mary G. Lockhart, and Edward H. Teets, "Atmospheric Analysis for Airdata Calibration on Research Aircraft," AIAA-92-0293, Jan. 1992.

[2]Maine, Richard E., "Flight Data Access System Programmer's Manual," NASA Dryden Internal Memo, Dec. 10, 1992.

[3]Pearson, Kermit E., Dennis D. Kasparek, and Lucile N. Tarrant, *The Refraction Correction Developed for the AN/FPS-16 Radar at White Sands Missile Range*, U.S. Army Signal Missile Support Agency, White Sands Missile Range, New Mexico, WSMR TM-577, Nov. 1958.

[4]James, Robert, *Baseline Mathematics and Geodetics for Tracking Operations*, NASA CR-163102, 1981.

[5]Lear, William M., *Computing Atmospheric Scale Height for Refraction Corrections*, NASA JSC Internal Note 80-FM-16, JSC-16462, 1980.

[6]Franklin, Gene F. and J. David Powell, *Digital Control of Dynamic Systems*, Reading: Addison-Wesley, 1980.

[7]Fletcher, Clive A.J., *Computational Techniques for Fluid Dynamics 1: Fundamental and General Techniques*, Berlin: Springer-Verlag, 1988.

[8]James, Robert and James D. Brownlow, *Mathematical Analysis Study for Radar Data Processing and Enhancement, Part I: Radar Data Analysis*, NASA CR-166616, 1985.

[9]Bate, Roger R., Donald D. Mueller, and Jerry E. White, *Fundamentals of Astrodynamics*, New York: Dover Publications, 1971.

[10]Hedgley, David R., Jr., *An Exact Transformation from Geocentric to Geodetic Coordinates for Non-Zero Altitudes*, NASA TR R-458, 1976.

[11]Thomas, George B., Jr., *Calculus and Analytic Geometry*, part 2, 4th ed., Reading: Addison-Wesley, 1969, pp. 528–530.

[12]Dickson, Leonard E., *New First Course in the Theory of Equations*, New York: Wiley & Sons, 1962.

[13]Smith, Ernest K., Jr., and Stanley Weintraub, "The Constants in the Equation for Atmospheric Refractive Index at Radio Frequencies," *Proc. IRE*, vol. 41, Aug. 1953, pp. 1035–1037.

[14]Parish, O. Owen, and Terrill W. Putnam, *Equations for the Determination of Humidity from Dewpoint and Psychrometric Data*, NASA TN D-8401, 1977.

[15]James, Robert and James D. Brownlow, *Mathematical Analysis Study for Radar Data Processing and Enhancement, Part II: Modeling of Propagation Path Errors*, NASA CR-166616, 1985.

[16]*U.S. Standard Atmosphere, 1976*, Washington: National Oceanic and Atmospheric Administration, National Aeronautics and Space Administration, and United States Air Force, 1976.

National Aeronautics and
Space Administration
Code JTT
Washington, D.C.
20546-0001
Official Business
Penalty for Private Use, $300